

S-wave heavy quarkonium spectrum with next-to-next-to-next-to-leading logarithmic accuracy

C. Anzai, D. Moreno and A. Pineda

*Grup de Física Teòrica, Dept. Física and IFAE-BIST, Universitat Autònoma de Barcelona,
E-08193 Bellaterra (Barcelona), Spain*

December 31, 2018

Abstract

We obtain the Potential NRQCD Lagrangian relevant for S-wave states with next-next-to-next-to-leading logarithmic (NNNLL) accuracy. We compute the heavy quarkonium mass of spin-averaged $l = 0$ (angular momentum) states, with otherwise arbitrary quantum numbers, with NNNLL accuracy. These results are complete up to a missing contribution of the two-loop soft running.

Contents

1	Introduction	2
2	NRQCD Lagrangian: $1/m^3$ and beyond	5
3	pNRQCD Lagrangian	6
4	NRQCD–pNRQCD matching, spin-independent	14
4.1	$\mathcal{O}(\alpha/m^4)$ potential	15
4.2	$\mathcal{O}(\alpha^2/m^3)$ potential	15
4.3	$\mathcal{O}(\alpha^3/m^2)$ V_r potential	19
4.4	Equations of motion	21
5	$\tilde{D}_d^{(2)}$ NLL running	23
5.1	Soft running	24
5.2	Ultrasoft running	28
5.3	Potential running	29
5.4	Potential running, spin-dependent delta potential	38
6	N^3LL heavy quarkonium mass	38
7	Conclusions	40
A	Matching scheme (in)dependence	41

1 Introduction

High order perturbative computations in heavy quarkonium require the use of effective field theories (EFTs), as they efficiently deal with the different scales of the system. One such EFT is Potential NRQCD (pNRQCD) [1, 2] (for reviews see [3, 4]). The key ingredient of the EFT is, obviously, its Lagrangian. At present the pNRQCD Lagrangian is known with next-to-next-to-next-to-leading order (NNNLO) accuracy [5] (for the nonequal mass case see [6]).

One of the major advantages of using EFTs is that it facilitates the systematic resummation of the large logarithms generated by the ratios of the different scales of the problem. For the case at hand we are talking of

- the hard scale (m , the heavy quark mass),
- the soft scale (mv , the inverse Bohr radius of the problem),
- and the ultrasoft scale (mv^2 , the typical binding energy of the system).

At present, the pNRQCD Lagrangian is known with next-to-next-to-next-to-leading log (N³LL) precision as far as P-wave states is concerned [7]. For S-wave observables the present precision is NNLL [8]. The missing link to obtain the complete N³LL pNRQCD Lagrangian is the N³LL running of the delta(-like) potentials¹. For the spin-dependent case, such precision for the running has already been achieved in [9, 10]. Therefore, what is left is to obtain the N³LL result for the spin-independent delta potential. This is an extremely challenging computation. We undertake this task in this paper.

The new results we obtain in this paper are the following:

- We compute the α/m^4 and the α^2/m^3 spin-independent potentials. These potentials are finite. The expectation value of them produce energy shifts of order $m\alpha^6$, which contribute to the heavy quarkonium mass at N³LO. Nevertheless, since some expectation values are divergent, some of these energy shifts are logarithmic enhanced, i.e. of order $\mathcal{O}(m\alpha^6 \ln(\frac{\nu}{m\alpha}))$. Such corrections contribute to the heavy quarkonium mass at N³LL. This divergence, and the associated factorization scale ν , gets canceled by the corresponding divergence in the spin-independent delta potential. By incorporating the HQET Wilson coefficients with LL accuracy² in the α/m^4 and α^2/m^3 spin-independent potentials, the divergent structure of their expectation value (tantamount to compute potential loops) determines the piece associated to these potentials of the renormalization group (RG) equation of the spin-independent delta potential with N³LL precision.
- We compute the (soft-) α^3/m^2 contribution to the spin-independent delta-like potential proportional to $[c_F^{(1)}]^2$, $[c_F^{(2)}]^2$, $\bar{c}_1^{(1)hl}$ and $\bar{c}_1^{(2)hl}$. Unlike before, this potential is divergent. Therefore, for future use, we also give the renormalized expression. The divergent pieces produce corrections of $\mathcal{O}(m\alpha^6 \ln(\frac{\nu}{m\alpha}))$ (i.e. of order N³LL). From these divergences we generate the (soft) RG equation of the spin-independent delta potential and resum logarithms with N³LL precision. In order to reach this accuracy, we need the NLL running of the $1/m^2$ HQET Wilson coefficients. For c_F this is known [15, 16] but not for \bar{c}_1^{hl} (the associated missing term is of $\mathcal{O}(T_f n_f m\alpha^6 \ln(1/\alpha))$ and is expected to be quite small. Its computation will be carried out elsewhere). The possible mixing between the (soft-) α^3/m^2 and the α^2/m^3 spin-independent potential computed in this paper is also quantified.

The computation of the (soft-) α^3/m^2 contribution to the spin-independent delta-like potential, proportional to other NRQCD Wilson coefficients, like $[c_k^{(1)}]^2$, $[c_k^{(2)}]^2$, and $c_k^{(1)} c_k^{(2)}$, will be performed in a separated paper. The associated contribution to the running is expected to be small in comparison with the total running of the heavy quarkonium potential. We will estimate its size using the result of the running of the already computed soft contribution.

¹We use the term “delta(-like) potentials” for the delta potential and the potentials generated by the Fourier transform of $\ln^n k$ (in practice only $\ln k$).

²These are known at $\mathcal{O}(1/m)$ [11], $\mathcal{O}(1/m^2)$ [12, 13] and $\mathcal{O}(1/m^3)$ [14].

- The N³LL ultrasoft running of the static, $1/m$ and $1/m^2$ potential was originally computed in [17, 18, 19] (see also [20, 21]). This is enough for P-wave analyses [7], where such corrections produce a N³LL shift to the energy. Nevertheless, it is not so for S-wave states, as already noted in [9, 10] for the case of the hyperfine splitting. The reason is the generation of singular potentials through divergent ultrasoft loops. We revisit it in Sec. 5.2 and incorporate the missing contributions needed to have the complete ultrasoft-potential running that produces N³LL shifts to the energy.
- Finally, we compute the complete (potential) RG equation of the delta potential with N³LL accuracy (the first nonzero contribution). Solving this equation we obtain the complete N³LL running of the delta potential. This allows us to obtain the S-wave mass with N³LL accuracy. It is also one of the missing blocks to obtain the complete NNLL RG improved expression of the Wilson coefficient of the electromagnetic current. This, indeed, is what is needed to achieve NNLL precision for non-relativistic sum rules and $t\bar{t}$ production near threshold. As the spin-dependent (and $l \neq 0$) contribution has already been computed in earlier papers [9, 10, 7], we only consider here energy averages of S-wave states where the spin-dependent contributions vanish, and only include terms relevant for the N³LL S-wave spin-average energy.

Throughout this paper we work in the $\overline{\text{MS}}$ renormalization scheme, where bare and renormalized coupling are related as ($D = 4 + 2\epsilon$)

$$g_B^2 = g^2 \left[1 + \frac{g^2 \bar{\nu}^{2\epsilon}}{(4\pi)^2} \beta_0 \frac{1}{\epsilon} + \left(\frac{g^2 \bar{\nu}^{2\epsilon}}{(4\pi)^2} \right)^2 \left[\beta_0^2 \frac{1}{\epsilon^2} + \beta_1 \frac{1}{\epsilon} \right] + \mathcal{O}(g^6) \right], \quad \bar{\nu}^{2\epsilon} = \nu^{2\epsilon} \left(\frac{e^{\gamma_E}}{4\pi} \right)^\epsilon, \quad (1)$$

where

$$\begin{aligned} \beta_0 &= \frac{11}{3} C_A - \frac{4}{3} T_F n_f, \\ \beta_1 &= \frac{34}{3} C_A^2 - \frac{20}{3} C_A T n_f - 4 C_F T n_f. \end{aligned} \quad (2)$$

n_f is the number of dynamical (active) quarks and $\alpha = g^2 \nu^{2\epsilon} / (4\pi)$. This definition is slightly different from the one used, for instance, in [22].

In the following we will only distinguish between the bare coupling g_B and the $\overline{\text{MS}}$ renormalized coupling g when necessary. The running of α is governed by the β function defined through

$$\frac{1}{2} \nu \frac{d}{d\nu} \frac{\alpha}{\pi} = \nu^2 \frac{d}{d\nu^2} \frac{\alpha}{\pi} = \beta(\alpha) = -\frac{\alpha}{\pi} \left\{ \beta_0 \frac{\alpha}{4\pi} + \beta_1 \left(\frac{\alpha}{4\pi} \right)^2 + \dots \right\}. \quad (3)$$

$\alpha(\nu)$ has n_f active light flavours and we define $z = \left[\frac{\alpha(\nu)}{\alpha(\nu_h)} \right]^{\frac{1}{\beta_0}} \simeq 1 - 1/(2\pi) \alpha(\nu_h) \ln(\frac{\nu}{\nu_h})$. Note that with the precision achieved in this paper we need in some cases the two-loop running of the coupling when solving the RG equations.

2 NRQCD Lagrangian: $1/m^3$ and beyond

Instrumental in the determination of the Wilson coefficients of the pNRQCD Lagrangian is the determination of the Wilson coefficients of the Lagrangian of the EFT named NRQCD [23, 24]. We first need to assess which NRQCD operators we have to include in our analysis. We will include light fermions, which we will take to be massless.

The HQET $1/m^3$ Lagrangian can be found in [25], and including light fermions, though in a different basis, in [26]. Here we use the basis and notation from [14], which also includes light fermions. In [14] one can find the resummed expressions of the Wilson coefficients with LL accuracy for the spin-independent operators. For the spin-dependent $1/m^3$ operators, not relevant for this work, the LL running can be found in [27, 28]. Note that there are no pure gluonic operators of dimension seven.

To obtain the complete $1/m^3$ NRQCD Lagrangian, one also has to consider possible dimension-seven four heavy-fermion operators. There are no such operators, as mentioned in [29]. At $\mathcal{O}(1/m^4)$, we do not need the complete Lagrangian for the purposes of this paper. For the heavy-quark bilinear sector the complete set of operators was written for the case of QED in [30] and for QCD in [31] (in the last case without light fermions). Of those we can neglect most, we do not need the spin-dependent $1/m^4$ operators, nor terms proportional to a single \mathbf{B} , nor terms with two (either \mathbf{B} or \mathbf{E}) terms. The reason is that we only need $1/m^4$ tree level potentials. Therefore, we can take all relevant operators from the QED case. Following the notation of [30], the possible relevant operators are

$$\delta\mathcal{L}_\psi^{(4)} = \frac{c_{X1}^{(1)}}{m_1^4} \psi^\dagger g[\mathbf{D}^2, \mathbf{D}\cdot\mathbf{E} + \mathbf{E}\cdot\mathbf{D}]\psi + \frac{c_{X2}^{(1)}}{m_1^4} \psi^\dagger g\{\mathbf{D}^2, [\nabla\cdot\mathbf{E}]\}\psi + \frac{c_{X3}^{(1)}}{m_1^4} \psi^\dagger g[\nabla^2, \nabla\cdot\mathbf{E}]\psi + \dots \quad (4)$$

and similarly for the antiquark. The dots stand for terms that one can trivially see that do not contribute to the S-wave spin-independent spectrum at NNNLL, either because involved the emission of two gluons or because they are spin-dependent. In principle we need three new coefficients. Nevertheless, we will see later that only c_{X1} contributes to the running of the spin-independent delta potential. Still, we will compute any tree level potential proportional to c_{X1} , c_{X2} and c_{X3} .

The fact that we need c_{X1} , one of the Wilson coefficients of the $1/m^4$ heavy quark bilinear Lagrangian, could make it necessary to consider the Wilson coefficients of the $1/m^4$ heavy-light operators as well [light-light operators are subleading for the same reason they are at $\mathcal{O}(1/m^3)$], as they may enter through RG mixing. Fortunately, c_{X1} can be determined by reparameterization invariance, which gives us the following relation [30]:

$$32c_{X1}^{(i)} = \frac{5Z}{4} - c_F^{(i)} + c_D^{(i)} \quad (5)$$

(where one should take $Z = 1$ for QCD). Note that it depends on c_D , so indeed $c_{X1}^{(i)}$ is gauge dependent. Nevertheless, we will see later that it always combines with c_M to produce gauge invariant combinations. This indeed is a nontrivial check of the computation. Note also that the above coefficient has an Abelian term, so it can be checked with QED computations.

Finally, we consider the heavy four-fermion sector of the $1/m^4$ Lagrangian. They generate local or quasi-local potentials, which do not produce divergent potential loops. The same happens for the potentials generated by c_{X2} , c_{X3} . Therefore, in both cases, such potentials do not generate contributions to the heavy quarkonium mass at N³LL, and we can neglect them.

Out of this discussion, we conclude that we have the LL running of all necessary Wilson coefficients of the $1/m^4$ NRQCD Lagrangian operators.

3 pNRQCD Lagrangian

Integrating out the soft modes in NRQCD we end up with the EFT named pNRQCD. The most general pNRQCD Lagrangian compatible with the symmetries of QCD that can be constructed with a singlet and an octet (quarkonium) field, as well as an ultrasoft gluon field to NLO in the multipole expansion has the form [1, 2]

$$\begin{aligned} \mathcal{L}_{\text{pNRQCD}} = & \int d^3\mathbf{r} \text{Tr} \left\{ S^\dagger (i\partial_0 - h_s(\mathbf{r}, \mathbf{p}, \mathbf{P}_{\mathbf{R}}, \mathbf{S}_1, \mathbf{S}_2)) S + O^\dagger (iD_0 - h_o(\mathbf{r}, \mathbf{p}, \mathbf{P}_{\mathbf{R}}, \mathbf{S}_1, \mathbf{S}_2)) O \right\} \\ & + V_A(r) \text{Tr} \{ O^\dagger \mathbf{r} \cdot g\mathbf{E} S + S^\dagger \mathbf{r} \cdot g\mathbf{E} O \} + \frac{V_B(r)}{2} \text{Tr} \{ O^\dagger \mathbf{r} \cdot g\mathbf{E} O + O^\dagger O \mathbf{r} \cdot g\mathbf{E} \} \\ & - \frac{1}{4} G_{\mu\nu}^a G^{\mu\nu a} + \sum_{i=1}^{n_f} \bar{q}_i i\not{D} q_i, \end{aligned} \quad (6)$$

$$h_s(\mathbf{r}, \mathbf{p}, \mathbf{P}_{\mathbf{R}}, \mathbf{S}_1, \mathbf{S}_2) = \frac{\mathbf{p}^2}{2m_r} + \frac{\mathbf{P}_{\mathbf{R}}^2}{2M} + V_s(\mathbf{r}, \mathbf{p}, \mathbf{P}_{\mathbf{R}}, \mathbf{S}_1, \mathbf{S}_2), \quad (7)$$

$$h_o(\mathbf{r}, \mathbf{p}, \mathbf{P}_{\mathbf{R}}, \mathbf{S}_1, \mathbf{S}_2) = \frac{\mathbf{p}^2}{2m_r} + \frac{\mathbf{P}_{\mathbf{R}}^2}{2M} + V_o(\mathbf{r}, \mathbf{p}, \mathbf{P}_{\mathbf{R}}, \mathbf{S}_1, \mathbf{S}_2), \quad (8)$$

where $iD_0 O \equiv i\partial_0 O - g[A_0(\mathbf{R}, t), O]$, $\mathbf{P}_{\mathbf{R}} = -i\nabla_{\mathbf{R}}$ for the singlet, $\mathbf{P}_{\mathbf{R}} = -i\mathbf{D}_{\mathbf{R}}$ for the octet (where the covariant derivative is in the adjoint representation), $\mathbf{p} = -i\nabla_{\mathbf{r}}$,

$$m_r = \frac{m_1 m_2}{m_1 + m_2} \quad (9)$$

and $M = m_1 + m_2$. We adopt the color normalization

$$S = S \mathbf{1}_c / \sqrt{N_c}, \quad O = O^a \mathbf{T}^a / \sqrt{T_F}, \quad (10)$$

for the singlet field $S(\mathbf{r}, \mathbf{R}, t)$ and the octet field $O^a(\mathbf{r}, \mathbf{R}, t)$. Here and throughout this paper we denote the quark-antiquark distance vector by \mathbf{r} , the center-of-mass position of the quark-antiquark system by \mathbf{R} , and the time by t .

Both h_s and the potential V_s are operators acting on the Hilbert space of a heavy quark-antiquark system in the singlet configuration.³ V_s (and V_o) can be Taylor expanded

³Therefore, in a more mathematical notation: $h \rightarrow \hat{h}$, $V_s(\mathbf{r}, \mathbf{p}) \rightarrow \hat{V}_s(\hat{\mathbf{r}}, \hat{\mathbf{p}})$. We will however avoid this notation in order to facilitate the reading.

in powers of $1/m$ (up to logarithms). At low orders we have

$$\begin{aligned}
V_s &= V^{(0)} + \frac{V^{(1)}}{m_r} + \frac{V_{\mathbf{L}^2}^{(2)} \mathbf{L}^2}{m_1 m_2 r^2} + \frac{1}{2m_1 m_2} \left\{ \mathbf{p}^2, V_{\mathbf{p}^2}^{(2)}(r) \right\} + \frac{V_r^{(2)}}{m_1 m_2} \\
&+ \frac{1}{m_1 m_2} V_{S^2}^{(1,1)}(r) \mathbf{S}_1 \cdot \mathbf{S}_2 + \frac{1}{m_1 m_2} V_{\mathbf{S}_{12}}^{(1,1)}(r) \mathbf{S}_{12}(\mathbf{r}) \\
&+ \frac{1}{m_1 m_2} V_{LS_1}^{(2)}(r) \mathbf{L} \cdot \mathbf{S}_1 + \frac{1}{m_1 m_2} V_{LS_2}^{(2)}(r) \mathbf{L} \cdot \mathbf{S}_2 + \mathcal{O}(1/m^3), \tag{11}
\end{aligned}$$

where, $\mathbf{S}_1 = \boldsymbol{\sigma}_1/2$, $\mathbf{S}_2 = \boldsymbol{\sigma}_2/2$, $\mathbf{L} \equiv \mathbf{r} \times \mathbf{p}$, and $\mathbf{S}_{12}(\mathbf{r}) \equiv \frac{3\mathbf{r} \cdot \boldsymbol{\sigma}_1 \mathbf{r} \cdot \boldsymbol{\sigma}_2}{r^2} - \boldsymbol{\sigma}_1 \cdot \boldsymbol{\sigma}_2$.

$V^{(0)}$ is known with N³LL accuracy [17, 18]. The N³LL result for the $1/m$ and $1/m^2$ momentum dependent potential is also known in different matching schemes [19, 32, 7]: on-shell, off-shell (Coulomb, Feynman) and Wilson. In terms of the original definitions used in these papers they read (in four dimensions)

$$V^{(1)} = V^{(1,0)}(r) = V^{(0,1)} \equiv -\frac{C_F C_A D^{(1)}}{4r^2}, \tag{12}$$

$$\frac{V_{\mathbf{L}^2}^{(2)}}{m_1 m_2} \equiv \frac{V_{\mathbf{L}^2}^{(2,0)}(r)}{m_1^2} + \frac{V_{\mathbf{L}^2}^{(0,2)}(r)}{m_2^2} + \frac{V_{\mathbf{L}^2}^{(1,1)}(r)}{m_1 m_2} \equiv \frac{C_F D_2^{(2)}}{2m_1 m_2 r}, \tag{13}$$

$$\frac{V_{\mathbf{p}^2}^{(2)}}{m_1 m_2} \equiv \frac{V_{\mathbf{p}^2}^{(2,0)}(r)}{m_1^2} + \frac{V_{\mathbf{p}^2}^{(0,2)}(r)}{m_2^2} + \frac{V_{\mathbf{p}^2}^{(1,1)}(r)}{m_1 m_2} \equiv -\frac{C_F D_1^{(2)}}{m_1 m_2 r}. \tag{14}$$

The spin-dependent and momentum-dependent potentials are also known with N³LL precision [7]. We use the following definitions in this paper (again we refer to [7]):

$$\frac{1}{m_1 m_2} V_{LS_1}^{(2)}(r) \equiv \left(\frac{1}{m_1^2} V_{LS}^{(2,0)}(r) + \frac{1}{m_1 m_2} V_{L_2 S_1}^{(1,1)}(r) \right) \equiv \frac{3C_F D_{LS_1}^{(2)}}{2m_1 m_2}, \tag{15}$$

$$\frac{1}{m_1 m_2} V_{LS_2}^{(2)}(r) \equiv \left(\frac{1}{m_2^2} V_{LS}^{(0,2)}(r) + \frac{1}{m_1 m_2} V_{L_1 S_2}^{(1,1)}(r) \right) \equiv \frac{3C_F D_{LS_2}^{(2)}}{2m_1 m_2}. \tag{16}$$

More delicate are $V_{S^2}^{(1,1)}$ and $V_r^{(2)}$, as their running is sensitive to potential loops, which are more efficiently computed in momentum space. Therefore, it is more convenient to work with the potential in momentum space, which is defined in the following way:

$$\tilde{V}_s \equiv \langle \mathbf{p}' | V_s | \mathbf{p} \rangle. \tag{17}$$

Then the potential reads

$$\begin{aligned}
\tilde{V}_s = & -4\pi C_F \frac{\alpha_{\tilde{V}}}{\mathbf{q}^2} - \mathbf{p}^4 \left(\frac{c_4^{(1)}}{8m_1^3} + \frac{c_4^{(2)}}{8m_2^3} \right) (2\pi)^d \delta^{(d)}(\mathbf{q}) \\
& - C_F C_A \tilde{D}^{(1)} \frac{\pi^2}{2m_r |\mathbf{q}|^{1-2\epsilon}} (1 + \mathcal{O}(\epsilon)) \\
& - \frac{2\pi C_F \tilde{D}_1^{(2)}}{m_1 m_2} \frac{\mathbf{p}^2 + \mathbf{p}'^2}{\mathbf{q}^2} + \frac{\pi C_F \tilde{D}_2^{(2)}}{m_1 m_2} \left(\left(\frac{\mathbf{p}^2 - \mathbf{p}'^2}{\mathbf{q}^2} \right)^2 - 1 \right) \\
& + \frac{\pi C_F \tilde{D}_d^{(2)}}{m_1 m_2} - \frac{4\pi C_F \tilde{D}_{S^2}^{(2)}}{d m_1 m_2} [\mathbf{S}_1^i, \mathbf{S}_1^j] [\mathbf{S}_2^i, \mathbf{S}_2^j] \\
& + \frac{4\pi C_F \tilde{D}_{S^{12}}^{(2)}}{d m_1 m_2} [\mathbf{S}_1^i, \mathbf{S}_1^r] [\mathbf{S}_2^i, \mathbf{S}_2^j] \left(\delta^{rj} - d \frac{\mathbf{q}^r \mathbf{q}^j}{\mathbf{q}^2} \right) \\
& - \frac{6\pi C_F}{m_1 m_2} \frac{\mathbf{p}^i \mathbf{q}^j}{\mathbf{q}^2} \left(\tilde{D}_{LS_1}^{(2)} [\mathbf{S}_1^i, \mathbf{S}_1^j] + \tilde{D}_{LS_2}^{(2)} [\mathbf{S}_2^i, \mathbf{S}_2^j] \right),
\end{aligned} \tag{18}$$

where the (Wilson) coefficients \tilde{D} generically stand for the Fourier transform of the original Wilson coefficients in position space D . For them (and for $\alpha_{\tilde{V}}$) we use the power counting LL/LO for the first nonvanishing correction, and so on.

$V_{S^2}^{(1,1)}$ is indeed known with the required N³LL accuracy [9, 10] (one should be careful when comparing though, as there is a change in the basis of potentials used there, compared with the one we use here). In terms of $\tilde{D}_{S^2}^{(2)}$ it reads

$$\begin{aligned}
\frac{V_{S^2}^{(1,1)}}{m_1 m_2} & \equiv \\
& \equiv \delta^{(3)}(\mathbf{r}) \frac{8\pi C_F \tilde{D}_{S^2}^{(2)}}{3m_1 m_2} + \frac{8\pi C_F \tilde{D}_{S^2}^{(2)}}{3m_1 m_2} \left[-\frac{1}{4\pi} \text{reg} \frac{1}{r^3} - \ln \nu \delta^{(3)}(\mathbf{r}) \right] \left(k \frac{d}{dk} \tilde{D}_{S^2}^{(2)} \right) \Bigg|_{k=\nu}^{LL}, \tag{19}
\end{aligned}$$

where

$$-\frac{1}{4\pi} \text{reg} \frac{1}{r^3} \equiv \int \frac{d^3 k}{(2\pi)^3} e^{-i\mathbf{k}\cdot\mathbf{r}} \ln k, \tag{20}$$

and we neglect higher order logarithms (as they are subleading).

Finally we consider V_r . In terms of $\tilde{D}_d^{(2)}$ it reads

$$\begin{aligned}
\frac{V_r^{(2)}}{m_1 m_2} & \equiv \frac{V_r^{(2,0)}(r)}{m_1^2} + \frac{V_r^{(0,2)}(r)}{m_2^2} + \frac{V_r^{(1,1)}(r)}{m_1 m_2} \\
& \equiv \delta^{(3)}(\mathbf{r}) \frac{\pi C_F \tilde{D}_d^{(2)}}{m_1 m_2} + \frac{\pi C_F}{m_1 m_2} \left[-\frac{1}{4\pi} \text{reg} \frac{1}{r^3} - \ln \nu \delta^{(3)}(\mathbf{r}) \right] \left(k \frac{d}{dk} \tilde{D}_d^{(2)} \right) \Bigg|_{k=\nu}^{LL}. \tag{21}
\end{aligned}$$

Unlike all the other potentials, we do not know $V_r^{(2)}$ with N³LL expression (though the N²LL expression is known [8]). This leads us to the main purpose of this paper: the computation of V_r with N³LL accuracy. This is equivalent to obtaining the NLL expression of $\tilde{D}_d^{(2)}$. This will require the use of the other Wilson coefficients to one order less: LL. Indeed in Eq. (18) we have already approximated the Fourier transform of $V_{\mathbf{L}^2}^{(2)}$ by its N²LL expression (otherwise the momentum dependence is more complicated).

At LL the Wilson coefficients are equal in position and momentum space. We only explicitly display those that we will need later. For the static potential we would have at LL that $\alpha_V = \alpha_{\tilde{V}} = \alpha$. For the rest, we show the results in the off-shell Coulomb (which are equal to the Feynman at this order) and on-shell matching schemes, except for $D_{LS_i}^{(2)}$, which we do not need for S-wave:

$$D_{CG}^{(1),LL} = \tilde{D}_{CG}^{(1),LL} = \alpha^2(\nu) + \frac{16}{3\beta_0} \left(\frac{C_A}{2} + C_F \right) \alpha^2(\nu) \ln \left(\frac{\alpha(\nu)}{\alpha(\nu^2/\nu_h)} \right), \quad (22)$$

$$D_{OS}^{(1),LL} = \tilde{D}_{OS}^{(1),LL} = \alpha^2(\nu) \left[1 - \frac{2C_F}{C_A} \frac{m_r^2}{m_1 m_2} \right] + \frac{16}{3\beta_0} \left(\frac{C_A}{2} + C_F \right) \alpha^2(\nu) \ln \left(\frac{\alpha(\nu)}{\alpha(\nu^2/\nu_h)} \right), \quad (23)$$

$$D_1^{(2),LL} = \tilde{D}_1^{(2),LL} = \alpha(\nu) + \frac{(m_1 + m_2)^2}{m_1 m_2} \frac{2C_A}{3\beta_0} \alpha(\nu) \ln \left(\frac{\alpha(\nu)}{\alpha(\nu^2/\nu_h)} \right), \quad (24)$$

$$D_{S_{12}}^{(2),LL} = \tilde{D}_{S_{12}}^{(2),LL} = \alpha(\nu) c_F^2(\nu), \quad (25)$$

$$D_{S^2}^{(2),LL} = \tilde{D}_{S^2}^{(2),LL} = \alpha(\nu) c_F^2(\nu) - \frac{3}{2\pi C_F} (d_{sv}(\nu) + C_F d_{vv}(\nu)). \quad (26)$$

We now turn to $\tilde{D}_d^{(2)}$. Expanding $\tilde{D}_d^{(2)}(k, \nu)$ in powers of $\ln k$, we obtain

$$\tilde{D}_d^{(2)}(k, \nu) = \tilde{D}_d^{(2)}(\nu_s, \nu_p, \nu_p^2/\nu_h) \Big|_{\nu_s=\nu_p=\nu} + k \frac{d}{dk} \tilde{D}_d^{(2)}(k, \nu) \Big|_{k=\nu} \ln \left(\frac{k}{\nu} \right) + \dots, \quad (27)$$

where we have made explicit the dependence on the different factorization scales.

So far we have not made explicit the dependence on $\nu_h \sim m$. Nevertheless, it will play an important role later, when solving the RG equations. Therefore, in the following, we

use the notation $\tilde{D}_d^{(2)}(\nu_s, \nu_p, \nu_p^2/\nu_h) \Big|_{\nu_s=\nu_p=\nu} \equiv \tilde{D}_d^{(2)}(\nu_h; \nu)$.

$\tilde{D}_d^{(2)}(\nu_h; \nu)$ can be written in several ways: as a sum of the LL ($\tilde{D}_d^{(2),LL}(\nu_h; \nu)$) term and the NLL ($\delta\tilde{D}_d^{(2),NLL}(\nu_h; \nu)$) correction, or as the sum of the initial condition ($\tilde{D}_d^{(2)}(\nu_h; \nu_h) \equiv \tilde{D}_d^{(2)}(\nu_h)$) at the hard scale and the running contribution ($\delta\tilde{D}_d^{(2)}(\nu_h; \nu)$ where $\delta\tilde{D}_d^{(2)}(\nu_h; \nu_h) = 0$):

$$\tilde{D}_d^{(2)}(\nu_h; \nu) = \tilde{D}_d^{(2)}(\nu_h) + \delta\tilde{D}_d^{(2)}(\nu_h; \nu) = \tilde{D}_d^{(2),LL}(\nu_h; \nu) + \delta\tilde{D}_d^{(2),NLL}(\nu_h; \nu). \quad (28)$$

This Wilson coefficient may depend on the matching scheme. Here we mainly consider the off-shell Coulomb gauge matching scheme. Still, for later discussion, we also give expressions in the on-shell matching scheme (see [6] for more details).

The LL running is known [8]:

$$D_{d,CG}^{(2)LL}(\nu) = \tilde{D}_{d,CG}^{(2)LL}(\nu) = 2\alpha(\nu) + \frac{1}{\pi C_F} [d_{ss}(\nu) + C_F \bar{d}_{vs}(\nu)] + \frac{(m_1 + m_2)^2}{m_1 m_2} \frac{8}{3\beta_0} \left(\frac{C_A}{2} - C_F \right) \alpha(\nu) \ln \left(\frac{\alpha(\nu)}{\alpha(\nu^2/\nu_h)} \right), \quad (29)$$

$$D_{d,OS}^{(2)LL}(\nu) = \tilde{D}_{d,OS}^{(2)LL}(\nu) = \alpha(\nu) + \frac{1}{\pi C_F} [d_{ss}(\nu) + C_F \bar{d}_{vs}(\nu)] + \frac{(m_1 + m_2)^2}{m_1 m_2} \frac{8}{3\beta_0} \left(\frac{C_A}{2} - C_F \right) \alpha(\nu) \ln \left(\frac{\alpha(\nu)}{\alpha(\nu^2/\nu_h)} \right), \quad (30)$$

where

$$\bar{d}_{vs} = \pi\alpha \frac{c_D^{(2)}}{2} \frac{m_1}{m_2} + \pi\alpha \frac{c_D^{(1)}}{2} \frac{m_2}{m_1} + d_{vs} \quad (31)$$

is a gauge invariant combination of NRQCD Wilson coefficients, for which its LL running can be found in [8]. In order to visualize the relative importance of the NLL corrections compared with the LL term, we plot the later in Fig. 1 in the Coulomb gauge⁴. For reference, in these and latter figures, we use the following numerical values for the heavy quark masses and α : $m_b = 4.73$ GeV, $\alpha(m_b) = 0.216547$, $m_c = 1.5$ GeV, $\alpha(m_c) = 0.348536$ and $\alpha(2m_b m_c / (m_b + m_c)) = 0.290758$. $\nu_h = m_b$ for bottomonium, $\nu_h = m_c$ for charmonium, and $\nu_h = 2m_r = 2m_b m_c / (m_b + m_c)$ for the B_c system.

From the LL result (using the ν_s independence of the potential at LO) one obtains

$$k \frac{d}{dk} \tilde{D}_{d,CG}^{(2)} \Big|_{k=\nu}^{LL}(\nu_h; \nu) = -\beta_0 \frac{\alpha^2}{\pi} + \frac{\alpha^2}{\pi} \left(2C_F - \frac{C_A}{2} \right) c_k^{(1)} c_k^{(2)} \quad (32)$$

$$+ \frac{\alpha^2}{\pi} \left[\frac{m_1}{m_2} \left(\frac{1}{3} T_f n_f \bar{c}_1^{hl(2)} - \frac{4}{3} (C_A + C_F) [c_k^{(2)}]^2 - \frac{5}{12} C_A [c_F^{(2)}]^2 \right) \right.$$

$$\left. + \frac{m_2}{m_1} \left(\frac{1}{3} T_f n_f \bar{c}_1^{hl(1)} - \frac{4}{3} (C_A + C_F) [c_k^{(1)}]^2 - \frac{5}{12} C_A [c_F^{(1)}]^2 \right) \right]$$

$$- \frac{(m_1 + m_2)^2}{m_1 m_2} \frac{4}{3} \left(\frac{C_A}{2} - C_F \right) \frac{\alpha^2}{\pi} \left[\ln \left(\frac{\alpha(\nu)}{\alpha(\nu^2/\nu_h)} \right) + 1 \right].$$

This term contributes to the N³LL energy shift of the spectrum.

⁴Unlike in the other plots, we use here the two-loop running for α . The effect is small.

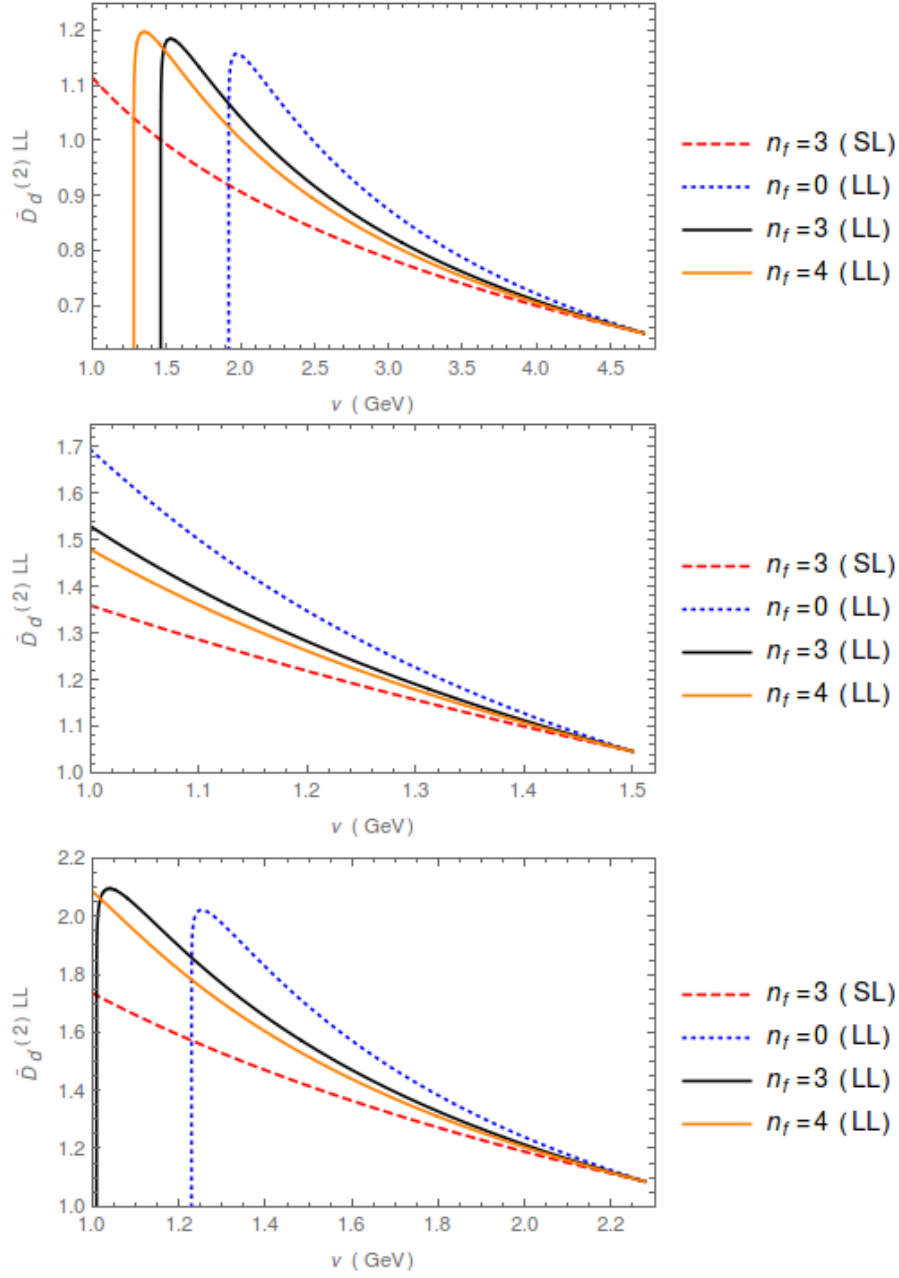


Figure 1: Plot of Eq. (29), the LL running in the off-shell (Coulomb/Feynman) matching scheme of $\tilde{D}_d^{(2)}$ for different values of n_f (0,3,4) and in the single log (SL) approximation (in this case only with $n_f = 3$). **Upper panel:** Plot for bottomonium with $\nu_h = m_b$. **Middle panel:** Plot for charmonium with $\nu_h = m_c$. **Lower panel:** Plot for B_c with $\nu_h = 2m_b m_c / (m_b + m_c)$.

Since we know the NLO expression of $\tilde{D}_d^{(2)}$, we can determine the initial matching

condition. It reads

$$\begin{aligned} \tilde{D}_{d,OS}^{(2)}(\nu_h) &= \alpha(\nu_h) + \frac{\alpha^2(\nu_h)}{4\pi} \left(\frac{28}{9}C_A + \frac{4}{3}C_F - \frac{20}{9}T_F n_f + \left(\frac{m_1}{m_2} + \frac{m_2}{m_1} \right) \left[\frac{25}{18}C_A - \frac{10}{9}T_F n_f \right] \right) \\ &\quad + \frac{1}{\pi C_F} (d_{ss}(\nu_h) + C_F \bar{d}_{vs}(\nu_h)) , \end{aligned} \quad (33)$$

$$\begin{aligned} \tilde{D}_{d,CG}^{(2)}(\nu_h) &= 2\alpha(\nu_h) + \frac{\alpha^2(\nu_h)}{4\pi} \left(\frac{62}{9}C_A + \frac{4}{3}C_F - \frac{32}{3}C_A \ln 2 - \frac{28}{9}T_F n_f \right. \\ &\quad \left. + \left(\frac{m_1}{m_2} + \frac{m_2}{m_1} \right) \left[-\frac{10}{9}T_F n_f + \left(\frac{61}{18} - \frac{16}{3} \ln 2 \right) C_A \right] \right) \\ &\quad + \frac{1}{\pi C_F} (d_{ss}(\nu_h) + C_F \bar{d}_{vs}(\nu_h)) . \end{aligned} \quad (34)$$

c_D , and the four-fermion Wilson coefficients d_{ss} and d_{vs} , were computed at one loop in [25] and [33] respectively, where one can find the explicit expressions.

At the order we are working $\delta \tilde{D}_d^{(2)NLL}(\nu_h; \nu)$ can be split into pieces. Thus, the NLL approximation for the Wilson coefficient is given by the sum

$$\begin{aligned} \delta \tilde{D}_d^{(2)NLL}(\nu_h; \nu) &= \left(\tilde{D}_d^{(2)} \right)_{1\text{-loop}}(\nu_h) \\ &\quad + \delta \tilde{D}_{d,us}^{(2)NLL}(\nu_h; \nu) + \delta \tilde{D}_{d,s}^{(2)NLL}(\nu_h; \nu) + \delta \tilde{D}_{d,p}^{(2)NLL}(\nu_h; \nu) , \end{aligned} \quad (35)$$

where the second line is zero when $\nu = \nu_h$. $\left(\tilde{D}_d^{(2)} \right)_{1\text{-loop}}(\nu_h)$ is the $\mathcal{O}(\alpha^2)$ term of Eq. (33) or (34), depending on the matching scheme. Their numerical values in the Coulomb gauge matching scheme are: for bottomonium 0.042, 0.052 and 0.081 for $n_f=4, 3$, and 0 respectively; for charmonium 0.108, 0.134 and 0.211 for $n_f=4, 3$, and 0 respectively; and for B_c 0.048, 0.072 and 0.142 for $n_f=4, 3$, and 0 respectively. We nicely observe that these numbers generate small corrections to the leading order results.

At present the NLL running is only known for the ultrasoft term [19]:

$$\begin{aligned} \delta \tilde{D}_{d,us}^{(2),NLL}(\nu_h; \nu) &= \frac{(m_1 + m_2)^2 4\pi}{m_1 m_2 \beta_0} \left(\frac{C_A}{2} - C_F \right) \alpha(\nu) \left\{ \frac{2}{3\pi} \ln \left(\frac{\alpha(\nu)}{\alpha(\nu^2/\nu_h)} \right) a_1 \frac{\alpha(\nu)}{4\pi} \right. \\ &\quad \left. + (\alpha(\nu^2/\nu_h) - \alpha(\nu)) \left(\frac{8}{3} \frac{\beta_1}{\beta_0} \frac{1}{(4\pi)^2} - \frac{1}{27\pi^2} (C_A (47 + 6\pi^2) - 10T_F n_f) \right) \right\} , \end{aligned} \quad (36)$$

where $a_1 = 31/9C_A - 20T_F n_f/9$. We show the size of this correction in Fig. 2. Note that the ultrasoft contribution to the delta potential vanishes in the large N_c limit (it is $1/N_c^2$ suppressed). Nevertheless, it quickly becomes big at relatively small scales because the overall coefficient is large and the ultrasoft scale quickly becomes small. Finally, note also that part of the ultrasoft correction (proportional to $\ln k$) is included in Eq. (32).

The missing terms to obtain the complete NLL running of $\tilde{D}_d^{(2)}$ are then $\delta \tilde{D}_{d,s}^{(2),NLL}(\nu_h; \nu)$ and $\delta \tilde{D}_{d,p}^{(2),NLL}(\nu_h; \nu)$. For $\delta \tilde{D}_{d,s}^{(2),NLL}(\nu_h; \nu)$ we need the two-loop soft computation of $\tilde{D}_d^{(2)}$,

in Secs. 4.1 and 4.2, an extra (ultrasoft associated) running, which we obtain in Sec. 5.2, and obtaining the potential RG equation, which we do in Sec. 5.3.

4 NRQCD–pNRQCD matching, spin-independent

In this section we compute the potentials for which their expectation values produce corrections to the spectrum of $\mathcal{O}(m\alpha^6)$. This means the $\mathcal{O}(\alpha/m^4)$, $\mathcal{O}(\alpha^2/m^3)$ and $\mathcal{O}(\alpha^3/m^2)$ potentials. Of them we mostly care about those that produce logarithmic enhanced contributions to the spectrum. Therefore, in particular, we do not need to consider the p^6/m^5 correction to the kinetic term, since it does not give an ultraviolet divergent correction. The $\mathcal{O}(\alpha/m^4)$ and $\mathcal{O}(\alpha^2/m^3)$ potentials are finite. Some of them can be traced back from the QED computation. We mainly compare with [34] (but one could also look into [35] for the equal mass case). Logarithmic enhanced corrections are produced by the divergences generated when inserting these potentials in potential loops. On the other hand the logarithmic enhanced contribution to the spectrum due to the $\mathcal{O}(\alpha^3/m^2)$ is not generated by potential loops but by the divergent structure of the potential itself, which we then refer to as soft running. This case will be discussed separately in Sec. 5.1.

The spin-dependent case was computed in [9, 10]. Explicit expressions for the potentials can be found in the Appendix of [36]. They produced corrections to the hyperfine splitting (but not to the fine splittings, as shown in [7]).

4.1 $\mathcal{O}(\alpha/m^4)$ potential

From a tree level computation (see the first diagram in Fig. 3) we obtain the complete (spin-independent) α/m^4 potentials in momentum space:

$$\begin{aligned}
\tilde{V}_{tree} = & -c_D^{(1)} c_D^{(2)} C_F \frac{g^2}{64m_1^2 m_2^2} \mathbf{k}^2 \\
& -C_F g^2 \left(\frac{c_{X1}^{(1)}}{m_1^4} + \frac{c_{X1}^{(2)}}{m_2^4} \right) \frac{(\mathbf{p}^2 - \mathbf{p}'^2)^2}{\mathbf{k}^2} \\
& -C_F g^2 \left(\frac{c_{X2}^{(1)}}{m_1^4} + \frac{c_{X2}^{(2)}}{m_2^4} \right) (\mathbf{p}^2 + \mathbf{p}'^2) \\
& -C_F g^2 \left(\frac{c_{X3}^{(1)}}{m_1^4} + \frac{c_{X3}^{(2)}}{m_2^4} \right) \mathbf{k}^2 \\
& +C_F \frac{g^2 c_k^{(1)2} c_k^{(2)2}}{16m_1^2 m_2^2} \frac{1}{\mathbf{k}^4} (\mathbf{p}^2 - \mathbf{p}'^2)^2 \left(2(\mathbf{p}^2 + \mathbf{p}'^2) - \mathbf{k}^2 - \frac{(\mathbf{p}^2 - \mathbf{p}'^2)^2}{\mathbf{k}^2} \right) \\
& +C_F \frac{g^2}{16m_1 m_2} \left(\frac{c_4^{(1)} c_k^{(2)}}{m_1^2} + \frac{c_4^{(2)} c_k^{(1)}}{m_2^2} \right) \frac{\mathbf{p}^2 + \mathbf{p}'^2}{\mathbf{k}^2} \left(2(\mathbf{p}^2 + \mathbf{p}'^2) - \mathbf{k}^2 - \frac{(\mathbf{p}^2 - \mathbf{p}'^2)^2}{\mathbf{k}^2} \right) \\
& -C_F \frac{g^2}{16m_1 m_2} \left(\frac{c_M^{(1)} c_k^{(2)}}{m_1^2} + \frac{c_M^{(2)} c_k^{(1)}}{m_2^2} \right) \left(\frac{(\mathbf{p}^2 - \mathbf{p}'^2)^2}{\mathbf{k}^2} - (\mathbf{p} + \mathbf{p}')^2 \right). \tag{37}
\end{aligned}$$

In this result we have already used the (full) equations of motion replacing [37]

$$k_0^2 \rightarrow -\frac{c_k^{(1)} c_k^{(2)} (\mathbf{p}^2 - \mathbf{p}'^2)^2}{4m_1 m_2}. \tag{38}$$

Such k_0^2 terms are generated by Taylor expanding in powers of the energy k_0 the denominator of the transverse gluon propagator.

Not all terms in Eq. (37) contribute to the NLL running of the delta potential. The ones that are local (or pseudo-local) do not contribute, as they do not produce potential loop divergences, since the expectation values of these potentials are proportional to $|\psi(0)|^2$ and/or (analytic) derivatives of it (kind of $\nabla^2 |\psi(0)|^2$), which are finite. This happens for instance for the potentials proportional to c_D^2 , c_{X2} and c_{X3} . It is also this fact that allows us to neglect $1/m^4$ potentials generated by dimension eight four-heavy fermion operators of the NRQCD Lagrangian.

As we have incorporated the LL running of the HQET Wilson coefficients, these potentials are already RG improved.

Note that with trivial modifications these potentials are also valid for QED.

4.2 $\mathcal{O}(\alpha^2/m^3)$ potential

We now compute the complete set of the $\mathcal{O}(\alpha^2/m^3)$ spin-independent potentials. We show the relevant topologies that contribute to the α^2/m^3 potential in Fig. 3. By properly

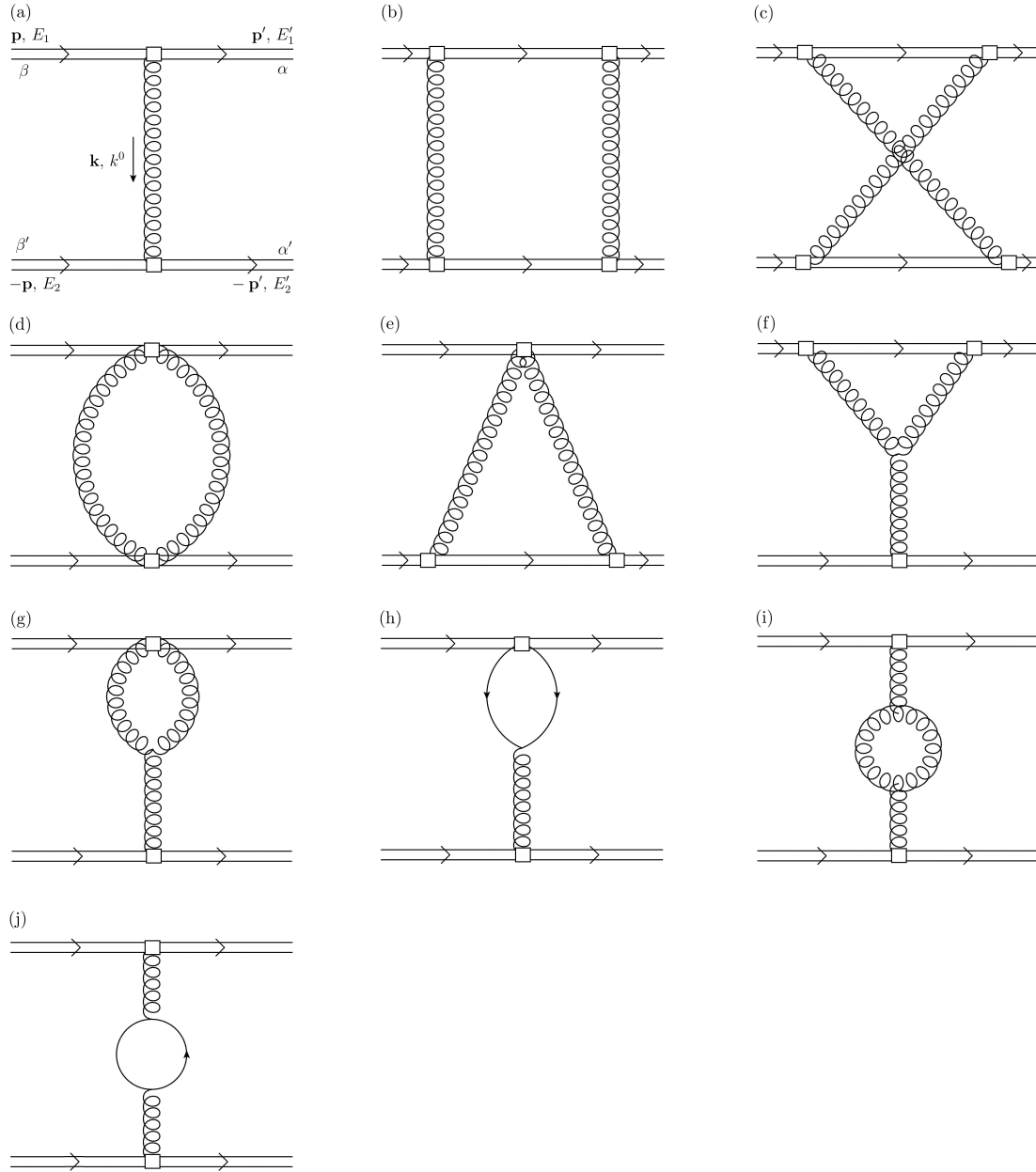


Figure 3: The first diagram is the only topology that contributes to the tree level potential. Properly changing the vertex and/or Taylor expanding the denominator of the propagators all potentials are generated. The other diagrams are the general topologies that contribute to the α^2/m^3 potential. Again, properly changing the vertices and/or Taylor expanding the denominator of the propagators, all potentials are generated.

changing the vertices all potentials are generated.

The (b) type diagrams in Fig. 3 do not generate $\mathcal{O}(\alpha^2/m^3)$ potentials (in the Coulomb

gauge).

The (c) type diagrams in Fig. 3 do generate $\mathcal{O}(\alpha^2/m^3)$ potentials. They read

$$\begin{aligned} \tilde{V}_{1loop}^{(c,1)} &= -C_F \left(C_F - \frac{C_A}{2} \right) c_k^{(1)} c_k^{(2)} \frac{g^4}{512m_1m_2} \frac{E_1 + E_2}{|\mathbf{k}|^{3-2\epsilon}} \\ &\quad \times \left(2(\mathbf{p}^2 + \mathbf{p}'^2) - \mathbf{k}^2 - \frac{(\mathbf{p}^2 - \mathbf{p}'^2)^2}{\mathbf{k}^2} - \frac{8(\mathbf{p} \cdot \mathbf{k})(\mathbf{p}' \cdot \mathbf{k})}{\mathbf{k}^2} \right), \end{aligned} \quad (39)$$

$$\begin{aligned} \tilde{V}_{1loop}^{(c,2)} &= -C_F \left(C_F - \frac{C_A}{2} \right) \frac{g^4}{256m_1m_2} \left(\frac{c_k^{(1)2} c_k^{(2)}}{m_1} + \frac{c_k^{(1)} c_k^{(2)2}}{m_2} \right) |\mathbf{k}|^{1+2\epsilon} \\ &\quad \times \left(3(\mathbf{p}^2 + \mathbf{p}'^2) \frac{(\mathbf{p} \cdot \mathbf{k})(\mathbf{p}' \cdot \mathbf{k})}{\mathbf{k}^6} - \frac{2(\mathbf{p}^2 + \mathbf{p}'^2)}{\mathbf{k}^2} + \frac{11}{4} - \frac{1}{4} \frac{(\mathbf{p}^2 - \mathbf{p}'^2)^2}{\mathbf{k}^4} - \frac{1}{2} \frac{(\mathbf{p}^2 + \mathbf{p}'^2)^2}{\mathbf{k}^4} \right). \end{aligned} \quad (40)$$

The (d) type diagrams in Fig. 3 do not generate $\mathcal{O}(\alpha^2/m^3)$ potentials.

The (e) type diagrams in Fig. 3 do generate $\mathcal{O}(\alpha^2/m^3)$ potentials. They read

$$\begin{aligned} \tilde{V}_{1loop}^{(e,1)} &= C_F \left(2C_F - \frac{C_A}{2} \right) \frac{g^4}{512m_1m_2} \left(\frac{c_k^{(1)2} c_k^{(2)}}{m_1} + \frac{c_k^{(1)} c_k^{(2)2}}{m_2} \right) |\mathbf{k}|^{1+2\epsilon} \\ &\quad \times \left(\frac{5(\mathbf{p}^2 + \mathbf{p}'^2)}{\mathbf{k}^2} - \frac{7}{2} - \frac{3}{2} \frac{(\mathbf{p}^2 - \mathbf{p}'^2)^2}{\mathbf{k}^4} \right), \end{aligned} \quad (41)$$

$$\begin{aligned} \tilde{V}_{1loop}^{(e,2)} &= -C_F \left(2C_F - \frac{C_A}{2} \right) \frac{g^4}{256} \left(\frac{c_{A1}^{(1)}}{m_1^3} + \frac{c_{A1}^{(2)}}{m_2^3} \right) |\mathbf{k}|^{1+2\epsilon} \\ &\quad - C_F \left(2C_F - \frac{C_A}{2} \right) \frac{g^4}{512} \left(\frac{c_{A2}^{(1)}}{m_1^3} + \frac{c_{A2}^{(2)}}{m_2^3} \right) |\mathbf{k}|^{1+2\epsilon} \\ &\quad - C_F \left(2C_F - \frac{C_A}{2} \right) \frac{g^4}{128m_1m_2} \left(\frac{c_F^{(1)2} c_k^{(2)}}{m_1} + \frac{c_F^{(2)2} c_k^{(1)}}{m_2} \right) |\mathbf{k}|^{1+2\epsilon} \\ &\quad - C_F C_A \frac{g^4}{256m_1m_2} \left(\frac{c_D^{(1)} c_k^{(2)}}{m_1} + \frac{c_D^{(2)} c_k^{(1)}}{m_2} \right) |\mathbf{k}|^{1+2\epsilon} \\ &\quad - \frac{T_F}{N_c} C_F \frac{g^4}{128} \left(\frac{c_{A3}^{(1)}}{m_1^3} + \frac{c_{A3}^{(2)}}{m_2^3} \right) |\mathbf{k}|^{1+2\epsilon} \\ &\quad - \frac{T_F}{N_c} C_F \frac{g^4}{256} \left(\frac{c_{A4}^{(1)}}{m_1^3} + \frac{c_{A4}^{(2)}}{m_2^3} \right) |\mathbf{k}|^{1+2\epsilon}. \end{aligned} \quad (42)$$

The (f) type diagrams in Fig. 3 do generate $\mathcal{O}(\alpha^2/m^3)$ potentials. They read

$$\tilde{V}_{1loop}^{(f,1)} = -C_F C_A \frac{g^4}{128} \left(\frac{c_F^{(1)2} c_k^{(1)}}{m_1^3} + \frac{c_F^{(2)2} c_k^{(2)}}{m_2^3} \right) |\mathbf{k}|^{1+2\epsilon} \frac{\mathbf{p} \cdot \mathbf{p}'}{\mathbf{k}^2}, \quad (43)$$

$$\begin{aligned}
\tilde{V}_{1loop}^{(f,2)} = & -C_F C_A \frac{g^4}{512 m_1 m_2} \left(\frac{c_k^{(2)} c_k^{(1)2}}{m_1} + \frac{c_k^{(1)} c_k^{(2)2}}{m_2} \right) |\mathbf{k}|^{1+2\epsilon} \left(1 - \frac{3\mathbf{p}^2 + \mathbf{p}'^2}{2\mathbf{k}^2} \right) \\
& \times \left(\frac{2(\mathbf{p}^2 + \mathbf{p}'^2)}{\mathbf{k}^2} - 1 - \frac{(\mathbf{p}^2 - \mathbf{p}'^2)^2}{\mathbf{k}^4} \right) \\
& - C_F C_A \frac{g^4}{512} \left(\frac{c_k^{(1)3}}{m_1^3} + \frac{c_k^{(2)3}}{m_2^3} \right) |\mathbf{k}|^{1+2\epsilon} \left(\frac{\mathbf{p} \cdot \mathbf{p}'}{\mathbf{k}^2} + \frac{5(\mathbf{p} \cdot \mathbf{k})(\mathbf{p}' \cdot \mathbf{k})}{\mathbf{k}^4} - \frac{12(\mathbf{p} \cdot \mathbf{p}')^2}{\mathbf{k}^4} + \frac{2\mathbf{p}^2 \mathbf{p}'^2}{\mathbf{k}^4} \right. \\
& \left. + \frac{6(\mathbf{p} \cdot \mathbf{p}')(\mathbf{p} \cdot \mathbf{k})(\mathbf{p}' \cdot \mathbf{k})}{\mathbf{k}^6} \right), \tag{44}
\end{aligned}$$

$$\begin{aligned}
\tilde{V}_{1loop}^{(f,3)} = & -c_k^{(1)} c_k^{(2)} C_F C_A \frac{3g^4}{128 m_1 m_2} |\mathbf{k}|^{-1+2\epsilon} \left(\mathbf{p} \cdot \mathbf{p}' - \frac{(\mathbf{p} \cdot \mathbf{k})(\mathbf{p}' \cdot \mathbf{k})}{\mathbf{k}^2} \right) \frac{(E_1 + E'_1) + (E_2 + E'_2)}{\mathbf{k}^2} \\
& - C_F C_A \frac{g^4}{256} \left(\frac{c_k^{(1)2}}{m_1^2} (E_1 + E'_1) + \frac{c_k^{(2)2}}{m_2^2} (E_2 + E'_2) \right) |\mathbf{k}|^{-1+2\epsilon} \left(\frac{5\mathbf{p} \cdot \mathbf{p}'}{\mathbf{k}^2} - \frac{3(\mathbf{p} \cdot \mathbf{k})(\mathbf{p}' \cdot \mathbf{k})}{\mathbf{k}^4} \right), \tag{45}
\end{aligned}$$

$$\begin{aligned}
\tilde{V}_{1loop}^{(f,4)} = & -C_F C_A \frac{g^4}{256} \left(\frac{c_k^{(1)3}}{m_1^3} + \frac{c_k^{(2)3}}{m_2^3} \right) |\mathbf{k}|^{1+2\epsilon} \left(-1 + \frac{\mathbf{p}^2 + \mathbf{p}'^2}{\mathbf{k}^2} \right. \\
& \left. + \frac{3(\mathbf{p}^4 + \mathbf{p}'^4) + (\mathbf{p}^2 + \mathbf{p}'^2)(\mathbf{p} \cdot \mathbf{p}') - 6(\mathbf{p} \cdot \mathbf{p}')^2}{\mathbf{k}^4} + \frac{-3(\mathbf{p}^6 + \mathbf{p}'^6) + 4(\mathbf{p}^4 + \mathbf{p}'^4)(\mathbf{p} \cdot \mathbf{p}') - 2(\mathbf{p} \cdot \mathbf{p}')^3}{\mathbf{k}^6} \right), \tag{46}
\end{aligned}$$

$$\begin{aligned}
\tilde{V}_{1loop}^{(f,5)} = & -C_F C_A \frac{g^4}{128} |\mathbf{k}|^{1+2\epsilon} \left[\frac{c_k^{(2)2}}{m_2^2} \left(\frac{3(E_1 + E'_1)(\mathbf{p} \cdot \mathbf{k})(\mathbf{p}' \cdot \mathbf{k})}{\mathbf{k}^6} + \frac{(E_1 + E'_1)(\mathbf{p} \cdot \mathbf{p}')}{\mathbf{k}^4} \right. \right. \\
& \left. \left. + \frac{2(E_1 \mathbf{p}^4 + E'_1 \mathbf{p}'^4)}{\mathbf{k}^6} - \frac{2(E_1 \mathbf{p}^2 + E'_1 \mathbf{p}'^2)(\mathbf{p} \cdot \mathbf{p}' + \mathbf{k}^2)}{\mathbf{k}^6} \right) + \frac{c_k^{(1)2}}{m_1^2} \left(\frac{3(E_2 + E'_2)(\mathbf{p} \cdot \mathbf{k})(\mathbf{p}' \cdot \mathbf{k})}{\mathbf{k}^6} \right. \right. \\
& \left. \left. + \frac{(E_2 + E'_2)(\mathbf{p} \cdot \mathbf{p}')}{\mathbf{k}^4} + \frac{2(E_2 \mathbf{p}^4 + E'_2 \mathbf{p}'^4)}{\mathbf{k}^6} - \frac{2(E_2 \mathbf{p}^2 + E'_2 \mathbf{p}'^2)(\mathbf{p} \cdot \mathbf{p}' + \mathbf{k}^2)}{\mathbf{k}^6} \right) \right], \tag{47}
\end{aligned}$$

$$\tilde{V}_{1loop}^{(f,6)} = -C_F C_A \frac{7g^4}{256 m_1 m_2} \left(\frac{c_k^{(1)2} c_k^{(2)}}{m_1} + \frac{c_k^{(1)} c_k^{(2)2}}{m_2} \right) |\mathbf{k}|^{1+2\epsilon} \left(\frac{2(\mathbf{p}^2 + \mathbf{p}'^2)}{\mathbf{k}^2} - 1 - \frac{(\mathbf{p}^2 - \mathbf{p}'^2)^2}{\mathbf{k}^4} \right), \tag{48}$$

$$\begin{aligned}
\tilde{V}_{1loop}^{(f,7)} = & C_F C_A \frac{g^4}{256 m_1 m_2} \left(\frac{c_D^{(1)} c_k^{(2)}}{m_1} + \frac{c_D^{(2)} c_k^{(1)}}{m_2} \right) |\mathbf{k}|^{1+2\epsilon} \\
& + C_F C_A \frac{g^4}{1024} \left(\frac{c_4^{(1)}}{m_1^3} + \frac{c_4^{(2)}}{m_2^3} \right) |\mathbf{k}|^{1+2\epsilon} \left(\frac{10(\mathbf{p}^2 + \mathbf{p}'^2)}{\mathbf{k}^2} - 7 + \frac{5(\mathbf{p}^2 - \mathbf{p}'^2)^2}{\mathbf{k}^4} \right) \\
& - C_F C_A \frac{g^4}{256} \left(\frac{c_M^{(1)}}{m_1^3} + \frac{c_M^{(2)}}{m_2^3} \right) |\mathbf{k}|^{1+2\epsilon} \\
& - C_F C_A \frac{g^4}{512} \left(\frac{c_F^{(1)} c_S^{(1)}}{m_1^3} + \frac{c_F^{(2)} c_S^{(2)}}{m_2^3} \right) |\mathbf{k}|^{1+2\epsilon}, \tag{49}
\end{aligned}$$

$$\tilde{V}_{1loop}^{(f,8)} = C_F C_A \frac{g^4}{64} |\mathbf{k}|^{-5+2\epsilon} \left[\left(c_k^{(1)} \frac{E_1^2}{m_1} + c_k^{(2)} \frac{E_2^2}{m_2} \right) (\mathbf{p} \cdot \mathbf{k}) - \left(c_k^{(1)} \frac{E_1'^2}{m_1} + c_k^{(2)} \frac{E_2'^2}{m_2} \right) (\mathbf{p}' \cdot \mathbf{k}) \right], \tag{50}$$

$$\tilde{V}_{1loop}^{(f,9)} = C_F C_A \frac{g^4}{128} \left(\frac{c_F^{(1)2}}{m_1^2} (E_1 + E_1') + \frac{c_F^{(2)2}}{m_2^2} (E_2 + E_2') \right) |\mathbf{k}|^{-1+2\epsilon}. \tag{51}$$

The rest of topologies ((g), (h), (i), (j)) do not contribute. Note that those topologies include, in particular, the one-loop diagrams proportional to c_i^{hl} or d_i^{hl} , as they may produce $\sim \alpha^2/m^3$ potentials. We find that such contributions vanish.

As we have incorporated the LL running of the HQET Wilson coefficients, these potentials are already RG improved.

Note that with trivial modifications these potentials are also valid for QED.

4.3 $\mathcal{O}(\alpha^3/m^2)$ V_r potential

In this section we perform a partial computation of the $\mathcal{O}(\alpha^3/m^2)$ soft contribution to the V_r potential. The contributions we compute here are those proportional to the HQET Wilson coefficients $\tilde{c}_1^{(i)hl}$ and $c_F^{(i)}$. We define

$$\frac{\tilde{D}_d^{(2)}}{m_1 m_2} = \frac{\tilde{D}_d^{(2,0)}}{m_1^2} + \frac{\tilde{D}_d^{(0,2)}}{m_2^2} + \frac{\tilde{D}_d^{(1,1)}}{m_1 m_2}. \tag{52}$$

Using the notation of [6],

$$\pi C_F \tilde{D}_{d,B}^{(2,0)} = \tilde{D}_r^{(2,0)} = g_B^2 C_F \left\{ D_{r,1}^{(2,0)} + \frac{g_B^2 k^{2\epsilon}}{16\pi^2} D_{r,2}^{(2,0)} + \frac{g_B^3 k^{4\epsilon}}{(4\pi)^3} D_{r,3}^{(2,0)} + \dots \right\}, \tag{53}$$

the bare new result reads

$$\begin{aligned}
\tilde{D}_{r,3}^{(2,0)} = & \bar{c}_1^{hl} \left[T_F n_l \left(C_A \left(-\frac{2^{-8\epsilon-4}\pi^{\frac{5}{2}-2\epsilon}3}{\epsilon(2\epsilon+3)\Gamma(2\epsilon+\frac{5}{2})} \right. \right. \right. \\
& - \frac{2^{-6\epsilon-3}\pi^{\frac{3}{2}-2\epsilon}(40\epsilon^4+160\epsilon^3+240\epsilon^2+167\epsilon+44)\csc(2\pi\epsilon)\Gamma^2(\epsilon+1)}{\epsilon(2\epsilon+3)\Gamma(\epsilon+\frac{5}{2})\Gamma(3\epsilon+3)} \\
& \left. \left. \left. + \frac{2^{-6\epsilon-3}\pi^{\frac{3}{2}-2\epsilon}(4\epsilon^4+12\epsilon^3+12\epsilon^2+13\epsilon+6)\sin(2\pi\epsilon)\csc^2(\pi\epsilon)\Gamma(-2\epsilon-3)\Gamma(\epsilon+2)}{\epsilon\Gamma(\epsilon+\frac{5}{2})} \right) \right. \\
& + C_F \left(\frac{2^{-8\epsilon-4}\pi^{2-2\epsilon}(2\epsilon+1)(2\epsilon+3)(\epsilon^2+2\epsilon+2)\csc(\pi\epsilon)\sec(\pi\epsilon)\Gamma(\epsilon+2)\Gamma(2\epsilon+2)}{\epsilon^2\Gamma^2(\epsilon+\frac{5}{2})\Gamma(3\epsilon+3)} \right. \\
& \left. \left. - \frac{2^{-8\epsilon-5}\pi^{3-2\epsilon}(\epsilon+1)(2\epsilon+3)(2\epsilon^2+\epsilon+2)\csc^2(\pi\epsilon)}{\epsilon\Gamma^2(\epsilon+\frac{5}{2})} \right) \right) + \frac{(T_F n_l)^2 2^{-8\epsilon-3}\pi^{3-2\epsilon}(\epsilon+1)^2 \csc^2(\pi\epsilon)}{\Gamma^2(\epsilon+\frac{5}{2})} \\
& + \left[c_F^{(1)} \right]^2 \frac{1}{3} C_A 2^{-8\epsilon-7}\pi^{-2\epsilon} \\
& \times \left[C_A \left(\frac{2^{4\epsilon+5}3(\epsilon(\epsilon(\epsilon(2\epsilon(18\epsilon(2\epsilon+11)+401)+661)+33)-283)-165)-30)\Gamma(1-2\epsilon)\Gamma^3(\epsilon)}{(4\epsilon(\epsilon+2)+3)^2\Gamma(3\epsilon+3)} \right. \right. \\
& + \frac{\pi^{24\epsilon+5}\Gamma(1-2\epsilon)\Gamma^3(\epsilon+\frac{1}{2})}{\Gamma(3\epsilon+\frac{3}{2})} + \frac{3\pi^3(\epsilon(\epsilon(22-\epsilon(12\epsilon+17))+45)+15)\csc^2(\pi\epsilon)}{\epsilon\Gamma^2(\epsilon+\frac{5}{2})} \\
& + \frac{24\pi^{5/2}(\epsilon(\epsilon(4\epsilon(\epsilon+12)+127)+130)+65)+15)\csc(\pi\epsilon)\csc(2\pi\epsilon)}{\epsilon(4\epsilon(\epsilon+2)+3)\Gamma(2\epsilon+\frac{5}{2})} + \frac{12\pi^4(2\epsilon-1)\sec^2(\pi\epsilon)}{\Gamma^2(\epsilon+1)} \\
& + \frac{24\pi^{3/2}n_f T_F}{(2\epsilon+3)^2} \left(\frac{4^{\epsilon+1}\Gamma(\epsilon+1)\left(\epsilon(4\epsilon+3)\cot(\pi\epsilon)\Gamma(-2\epsilon-1) - \frac{(6\epsilon^2+9\epsilon+4)(2\epsilon(2\epsilon+5)+5)\csc(2\pi\epsilon)\Gamma(\epsilon)}{\Gamma(3\epsilon+3)}\right)}{\Gamma(\epsilon+\frac{3}{2})} \right. \\
& \left. \left. - \frac{\pi(2\epsilon+1)^2(2\epsilon+3)\csc(\pi\epsilon)\csc(2\pi\epsilon)}{\Gamma(2\epsilon+\frac{5}{2})} \right) \right]. \tag{54}
\end{aligned}$$

With obvious changes the same result is obtained for $\tilde{D}_{r,3}^{(0,2)}$. It is worth emphasizing that this expression vanishes in pure QED. A non trivial check of this result is that c_D and c_1^{hl} appear in the gauge invariant combination $\bar{c}_1^{hl} = c_D + c_1^{hl}$. Another nontrivial check is that the counterterm is independent of k and that the $1/\epsilon^2$ terms comply with the constraints from RG. This computation has been done in the Feynman gauge (with a general gauge parameter ξ) in the kinematic configuration $\mathbf{p} = \mathbf{k}$ and $\mathbf{p}' = 0$. We also set the external energy to zero. Not setting it to zero produces subleading corrections (we recall that the one-loop computation of this contribution has no energy dependence [6]). The result is shown to be independent of the gauge fixing parameter ξ .

For future computations, it is useful to explain the convention we have taken for the D -dimensional spin matrices. For the $c_F^{(i)}$ vertex we typically take a covariant notation

$\sim \sigma^{\mu\nu}$ (see for instance [38]) and project to the particle to single out the spin-independent part: $\sim Tr[(I + \gamma_0)/2(\dots)(I + \gamma_0)/2]$. At one loop this procedure gives the same result than using Pauli matrices with the conventions used in [6].

Though not directly relevant for this work, we also give the $\overline{\text{MS}}$ renormalized expression of the bare potential computed above. It will be of relevance for future computations of the spectrum (and decays) at N⁴LO. The result reads ($\alpha = \alpha(\nu)$)

$$\begin{aligned}
\tilde{D}_{r,\overline{\text{MS}}}^{(2,0)}(\mathbf{k}) &= \frac{C_F \alpha^2}{2} \left[\frac{13}{36} c_F^{(1)2} C_A - \frac{5}{9} \tilde{c}_1^{hl(1)} T_F n_f + \left(-C_A \frac{5}{6} c_F^{(1)2} + \frac{2}{3} \tilde{c}_1^{hl(1)} T_F n_f \right) \ln(k/\nu) \right] \\
&+ c_F^{(1)2} C_F C_A^2 \frac{\alpha^3}{2\pi} \left(\frac{1080\zeta(3) + 706 - 900\gamma + 432\pi^2 - 81\pi^4 + 900 \ln(4\pi)}{5184} \right. \\
&\quad \left. - \frac{179}{108} \ln(k/\nu) + \frac{10}{9} \ln^2(k/\nu) \right) \\
&+ c_F^{(1)2} C_F C_A n_f T_F \frac{\alpha^3}{2\pi} \left(\frac{-3581 + 750\gamma - 750 \ln(4\pi)}{2592} + \frac{91}{54} \ln(k/\nu) - \frac{7}{12} \ln^2(k/\nu) \right) \\
&+ \tilde{c}_1^{hl} C_F n_f T_F C_A \frac{\alpha^3}{2\pi} \left(\frac{-1008\zeta(3) + 627 - 130\gamma + 130 \ln(4\pi)}{864} \right. \\
&\quad \left. + \frac{5}{6} \ln(k/\nu) - \frac{31}{36} \ln^2(k/\nu) \right) \\
&+ \tilde{c}_1^{hl} C_F^2 n_f T_F \frac{\alpha^3}{2\pi} \left(\frac{48\zeta(3) - 55 + 6\gamma - 6 \ln(4\pi)}{48} + \frac{1}{2} \ln(k/\nu) \right) \\
&+ \tilde{c}_1^{hl} C_F n_f^2 T_F^2 \frac{\alpha^3}{2\pi} \left(\frac{25}{81} - \frac{20}{27} \ln(k/\nu) + \frac{4}{9} \ln^2(k/\nu) \right), \tag{55}
\end{aligned}$$

where we have also included the $\mathcal{O}(\alpha^2)$ term. Note that this contribution does not mix with $V_{\mathbf{L}}^{(2)}$. Therefore, it really corresponds to the contributions proportional to $c_F^{(1)}$ and $\tilde{c}_1^{hl(1)}$ of $D_r^{(2,0)}$, as defined in [6]. With obvious changes a similar expression is obtained for $\tilde{D}_{r,\overline{\text{MS}}}^{(0,2)}(\mathbf{k})$.

Finally, note that the missing part of the soft term should carefully be computed in a way consistent with the scheme we have used for the rest of the computation, in particular of the α^2/m^3 potential, as a strong mixing (if using field redefinitions) of the terms proportional to c_k^2 is expected.

4.4 Equations of motion

Some of the potentials we have obtained in Sec. 4.2 are energy dependent. If we want to eliminate such energy dependence, and write an energy independent potential, this could be achieved by using field redefinitions. At the order we are working it is enough to use the full equation of motion (at leading order), which includes the Coulomb potential. Let us see how it works. We first consider Eq. (39). It depends on the total energy of the heavy quarkonium and does not contribute to the running of the delta potential. We

next consider Eq. (51), which is the only energy dependent potential proportional to $c_F^{(i)2}$. Such potential is generated by the following interaction Lagrangian

$$\begin{aligned}
L_{\tilde{V}_{1loop}^{(f,9)}} &= -C_F C_A \frac{g^4}{128} \frac{c_F^{(1)2}}{m_1^2} \int d^3 x_1 d^3 x_2 (\psi^\dagger (i\partial_0 \psi(t, \mathbf{x}_1)) - (i\partial_0 \psi^\dagger) \psi(t, \mathbf{x}_1)) \int \frac{d^3 k}{(2\pi)^3} \frac{e^{i\mathbf{k}\cdot\mathbf{x}}}{|\mathbf{k}|^{1-2\epsilon}} \chi_c^\dagger \chi_c(t, \mathbf{x}_2) \\
&- C_F C_A \frac{g^4}{128} \frac{c_F^{(2)2}}{m_2^2} \int d^3 x_1 d^3 x_2 \psi^\dagger \psi(t, \mathbf{x}_1) \int \frac{d^3 k}{(2\pi)^3} \frac{e^{i\mathbf{k}\cdot\mathbf{x}}}{|\mathbf{k}|^{1-2\epsilon}} (\chi_c^\dagger i\partial_0 \chi_c(t, \mathbf{x}_2) - (i\partial_0 \chi_c^\dagger) \chi_c(t, \mathbf{x}_2)).
\end{aligned} \tag{56}$$

For this Lagrangian one can use the equations of motion ($V_C(\mathbf{x}) = -C_F \alpha / |\mathbf{x}|$):

$$\left(i\partial_0 + \frac{\nabla^2}{2m_1} \right) \psi(t, \mathbf{x}) - \int d^3 x_2 \psi(t, \mathbf{x}) V_C(\mathbf{x} - \mathbf{x}_2) \chi_c^\dagger \chi_c(t, \mathbf{x}_2) = 0 \tag{57}$$

and similarly for the other fields. We then obtain

$$\begin{aligned}
L_{\tilde{V}_{1loop}^{(f,9)}} &= -C_F C_A \frac{g^4}{128} \frac{c_F^{(1)2}}{m_1^2} \int d^3 x_1 d^3 x_2 \left[\psi^\dagger \left(-\frac{\nabla^2}{2m_1} \psi(t, \mathbf{x}_1) \right) + \left(-\frac{\nabla^2}{2m_1} \psi^\dagger \right) \psi(t, \mathbf{x}_1) \right] \\
&\quad \times \int \frac{d^3 k}{(2\pi)^3} \frac{e^{i\mathbf{k}\cdot\mathbf{x}}}{|\mathbf{k}|^{1-2\epsilon}} \chi_c^\dagger \chi_c(t, \mathbf{x}_2) \\
&- C_F C_A \frac{g^4}{64} \frac{c_F^{(1)2}}{m_1^2} \int d^3 x_1 d^3 x_2 d^3 x_3 \psi^\dagger \psi(t, \mathbf{x}_1) V_C(\mathbf{x}_1 - \mathbf{x}_3) \\
&\quad \times \int \frac{d^3 k}{(2\pi)^3} \frac{e^{i\mathbf{k}\cdot(\mathbf{x}_1 - \mathbf{x}_2)}}{|\mathbf{k}|^{1-2\epsilon}} \chi_c^\dagger \chi_c(t, \mathbf{x}_2) \chi_c^\dagger \chi_c(t, \mathbf{x}_3) + \dots,
\end{aligned} \tag{58}$$

where the dots stand for the analogous contribution for the antiparticle.

The first term in Eq. (58) yields the potential we had obtained after using the free on-shell equations of motion in Eq. (51). It reads

$$\tilde{V}_{1loop}^{(f,9)} = C_F C_A \frac{g^4}{256} \left(\frac{c_F^{(1)2} c_k^{(1)}}{m_1^3} + \frac{c_F^{(2)2} c_k^{(2)}}{m_2^3} \right) |\mathbf{k}|^{1+2\epsilon} \frac{\mathbf{P}^2 + \mathbf{P}'^2}{\mathbf{k}^2}. \tag{59}$$

The second term is a six-fermion field term. After contracting two of them, a new α^3/m^2 potential is generated (here we only care about the divergent part). It reads

$$\delta \tilde{V}_{1loop}^{(f,9)} = \frac{1}{32\epsilon} C_F^2 C_A \frac{g^6 k^{4\epsilon}}{(4\pi)^2} \left[\frac{c_F^{(1)2}}{m_1^2} + \frac{c_F^{(2)2}}{m_2^2} \right]. \tag{60}$$

It is worth mentioning that this contribution has a different color structure as those (purely soft) computed in Sec. 4.3, and that they are π^2 enhanced compared to those also. Therefore, one could expect them to be more important than the strict pure-soft contribution.

Remarkably enough, we will see later that the contributions from Eq. (59) and Eq. (60) to the running of the delta potential cancel each other in the equal mass case (but not for different masses). This was to be expected, since in the equal mass case, the potential can be written in terms of the total energy of the heavy quarkonium, which does not produce divergences that should be absorbed in the delta potential.

It is worth mentioning that this exhausts all possible $c_F^{(i)2}$ structures that can be generated. To be sure of this statement, we have to check that the result does not depend on the gauge. Therefore, we have redone the diagrams proportional to $c_F^{(i)2}$ (i.e. the associated contributions to $\tilde{V}_{1loop}^{(e,2)}$, $\tilde{V}_{1loop}^{(f,1)}$ and $\tilde{V}_{1loop}^{(f,9)}$) in the Feynman gauge and found the same result.

The other potentials that are dependent on the energy are proportional to c_k^2 . As before, these contributions will mix with the α^3/m^2 pure-soft contribution proportional to c_k^2 , which we have not computed anyhow. Therefore, in this paper, we only include the explicit contribution generated using the free equations of motion and postpone the incorporation of the other contribution to have the full result. The contributions we explicitly include in this paper then read:

$$\begin{aligned} \tilde{V}_{1loop}^{(f,3)} = & -C_F C_A \frac{3g^4}{1024m_1m_2} \left(\frac{c_k^{(1)2}c_k^{(2)}}{m_1} + \frac{c_k^{(1)}c_k^{(2)2}}{m_2} \right) |\mathbf{k}|^{1+2\epsilon} \frac{\mathbf{p}^2 + \mathbf{p}'^2}{\mathbf{k}^2} \left(\frac{2(\mathbf{p}^2 + \mathbf{p}'^2)}{\mathbf{k}^2} - 1 - \frac{(\mathbf{p}^2 - \mathbf{p}'^2)^2}{\mathbf{k}^4} \right) \\ & - C_F C_A \frac{g^4}{512} \left(\frac{c_k^{(1)3}}{m_1^3} + \frac{c_k^{(2)3}}{m_2^3} \right) |\mathbf{k}|^{1+2\epsilon} \frac{\mathbf{p}^2 + \mathbf{p}'^2}{\mathbf{k}^2} \left(\frac{5\mathbf{p} \cdot \mathbf{p}'}{\mathbf{k}^2} - \frac{3(\mathbf{p} \cdot \mathbf{k})(\mathbf{p}' \cdot \mathbf{k})}{\mathbf{k}^4} \right), \end{aligned} \quad (61)$$

$$\begin{aligned} \tilde{V}_{1loop}^{(f,5)} = & -C_F C_A \frac{g^4}{256m_1m_2} |\mathbf{k}|^{1+2\epsilon} \left(\frac{c_k^{(1)2}c_k^{(2)}}{m_1} + \frac{c_k^{(1)}c_k^{(2)2}}{m_2} \right) \left(\frac{3(\mathbf{p}^2 + \mathbf{p}'^2)(\mathbf{p} \cdot \mathbf{k})(\mathbf{p}' \cdot \mathbf{k})}{\mathbf{k}^6} \right. \\ & \left. - \frac{2(\mathbf{p}^4 + \mathbf{p}'^4)}{\mathbf{k}^4} + \frac{(\mathbf{p}^2 + \mathbf{p}'^2)(\mathbf{p} \cdot \mathbf{p}')}{\mathbf{k}^4} + \frac{2(\mathbf{p}^6 + \mathbf{p}'^6)}{\mathbf{k}^6} - \frac{2(\mathbf{p}^4 + \mathbf{p}'^4)(\mathbf{p} \cdot \mathbf{p}')}{\mathbf{k}^6} \right), \end{aligned} \quad (62)$$

$$\tilde{V}_{1loop}^{(f,8)} = C_F C_A \frac{g^4}{512} \left(\frac{c_k^{(1)3}}{m_1^3} + \frac{c_k^{(2)3}}{m_2^3} \right) |\mathbf{k}|^{1+2\epsilon} \left(\frac{2(\mathbf{p}^6 + \mathbf{p}'^6)}{\mathbf{k}^6} - \frac{(\mathbf{p}^4 + \mathbf{p}'^4)(\mathbf{p}^2 + \mathbf{p}'^2)}{\mathbf{k}^6} + \frac{\mathbf{p}^4 + \mathbf{p}'^4}{\mathbf{k}^4} \right). \quad (63)$$

5 $\tilde{D}_d^{(2)}$ NLL running

We now compute the NLL soft and potential running of $\tilde{D}_d^{(2)}$.

5.1 Soft running

From the results obtained in Sec. 4.3 we can obtain the $\mathcal{O}(\alpha^3)$ RG soft equation of \tilde{D}_d (the $\mathcal{O}(\alpha^2)$ RG soft equation can be found in [8]) proportional to $c_F^{(i)2}$ and $c_1^{hl(i)}$. In practice, such computation can be understood as getting the NLL soft running of $d_{ss} + C_F \bar{d}_{vs}$ (see Eq. (29) or Eq. (30)). It reads

$$\begin{aligned}
\nu_s \frac{d}{d\nu_s} (d_{ss} + C_F \bar{d}_{vs}) \Big|_{soft} &= C_F \alpha^2 \left(2C_F - \frac{C_A}{2} \right) c_k^{(1)} c_k^{(2)} \\
&+ C_F \alpha^2 \left[\frac{m_1}{m_2} \left(\frac{1}{3} T_f n_f \bar{c}_1^{hl(2)} - \frac{4}{3} (C_A + C_F) [c_k^{(2)}]^2 - \frac{5}{12} C_A [c_F^{(2)}]^2 \right) \right. \\
&\quad \left. + \frac{m_2}{m_1} \left(\frac{1}{3} T_f n_f \bar{c}_1^{hl(1)} - \frac{4}{3} (C_A + C_F) [c_k^{(1)}]^2 - \frac{5}{12} C_A [c_F^{(1)}]^2 \right) \right] \\
&+ C_F \frac{\alpha^3}{4\pi} \left[\frac{m_1}{m_2} \left(-\frac{T_f n_f}{54} (65C_A - 54C_F) \bar{c}_1^{hl(2)} - \frac{C_A}{18} (25C_A - \frac{125}{3} T_f n_f) [c_F^{(2)}]^2 \right) \right. \\
&\quad \left. + \frac{m_2}{m_1} \left(-\frac{T_f n_f}{54} (65C_A - 54C_F) \bar{c}_1^{hl(1)} - \frac{C_A}{18} (25C_A - \frac{125}{3} T_f n_f) [c_F^{(1)}]^2 \right) \right] \\
&+ \mathcal{O}(\alpha^3).
\end{aligned} \tag{64}$$

The $\mathcal{O}(\alpha^3)$ stands for terms proportional to NRQCD Wilson coefficients different from $c_F^{(i)2}$ and $c_1^{hl(i)}$. This equation is meant to represent the pure soft running of the NRQCD Wilson coefficients. It does not give the full running of $\tilde{D}_d^{(2)}$, as one should also include the potential and ultrasoft running. We fix the initial matching condition to zero, since we only need the initial matching condition of the total potential, which can be determined in the final step, when combining the different contributions.

The strict NLL contribution to the solution of this equation reads (the LL is already

included in Eq. (29))

$$\begin{aligned}
\pi C_F \delta D_{d,s}^{(2),NLL} &= [d_{ss} + C_F \bar{d}_{vs}]^{NLL} = -\alpha^2(\nu_h) C_F \left[\left(465 C_A^6 (757 m_1^2 - 306 m_1 m_2 + 757 m_2^2) \right. \right. \\
&- 13824 C_F^2 (2 m_1^2 - 3 m_1 m_2 + 2 m_2^2) n_f^4 T_F^4 + C_A^5 \left(5580 C_F (53 m_1^2 + 102 m_1 m_2 + 53 m_2^2) \right. \\
&+ (-590218 m_1^2 + 342117 m_1 m_2 - 590218 m_2^2) n_f T_F \left. \right) - C_A^4 n_f T_F \left(34 C_F (8347 m_1^2 + 38772 m_1 m_2 \right. \\
&+ 8347 m_2^2) - 3 (115117 m_1^2 - 101466 m_1 m_2 + 115117 m_2^2) n_f T_F \left. \right) + 32 C_A n_f^3 T_F^3 \left(81 C_F^2 (70 m_1^2 \right. \\
&- 83 m_1 m_2 + 70 m_2^2) - 4 C_F (5 m_1^2 - 459 m_1 m_2 + 5 m_2^2) n_f T_F + 120 (m_1^2 + m_2^2) n_f^2 T_F^2 \left. \right) \\
&- 8 C_A^2 n_f^2 T_F^2 \left(81 C_F^2 (566 m_1^2 - 563 m_1 m_2 + 566 m_2^2) - 3 C_F (193 m_1^2 - 17595 m_1 m_2 + 193 m_2^2) n_f T_F \right. \\
&+ 2 (739 m_1^2 + 1080 m_1 m_2 + 739 m_2^2) n_f^2 T_F^2 \left. \right) + 6 C_A^3 n_f T_F \left(360 C_F^2 (106 m_1^2 - 93 m_1 m_2 + 106 m_2^2) \right. \\
&+ C_F (10129 m_1^2 + 187731 m_1 m_2 + 10129 m_2^2) n_f T_F - 4 (2536 m_1^2 - 4959 m_1 m_2 + 2536 m_2^2) n_f^2 T_F^2 \left. \right) \left. \right) \\
&\times \frac{1}{36 m_1 m_2 (31 C_A - 16 n_f T_F) (5 C_A - 4 n_f T_F) (11 C_A - 4 n_f T_F)^2 (2 C_A - n_f T_F)} \\
&+ 5 C_A (m_1^2 + m_2^2) \left(397 C_A^3 + 48 C_F n_f^2 T_F^2 + 11 C_A^2 (33 C_F - 35 n_f T_F) + 10 C_A n_f T_F (-21 C_F \right. \\
&+ 10 n_f T_F) \left. \right) z^{\frac{1}{3}(5 C_A - 4 n_f T_F)} \frac{1}{6 m_1 m_2 (5 C_A - 4 n_f T_F) (11 C_A - 4 n_f T_F)^2} \\
&- \frac{1}{468 m_1 m_2 (11 C_A - 4 n_f T_F)^2} \left(1989 C_A^3 (8 m_1^2 + 3 m_1 m_2 + 8 m_2^2) + 8 C_F n_f T_F \left(81 C_F (6 m_1^2 \right. \right. \\
&+ 13 m_1 m_2 + 6 m_2^2) + 1240 (m_1^2 + m_2^2) n_f T_F \left. \right) + 2 C_A n_f T_F \left(C_F (-15134 m_1^2 + 5967 m_1 m_2 \right. \\
&- 15134 m_2^2) + 3100 (m_1^2 + m_2^2) n_f T_F \left. \right) + 2 C_A^2 \left(3978 C_F (2 m_1^2 - 3 m_1 m_2 + 2 m_2^2) - 5 (2263 m_1^2 \right. \\
&+ 351 m_1 m_2 + 2263 m_2^2) n_f T_F \left. \right) \left. \right) z^{\frac{2}{3}(11 C_A - 4 n_f T_F)} \\
&+ \frac{2(5 C_A + 8 C_F)(m_1^2 + m_2^2) n_f T_F (-1327 C_A + 594 C_F + 620 n_f T_F) z^{\frac{31}{6} C_A - \frac{8}{3} n_f T_F}}{117 m_1 m_2 (31 C_A - 16 n_f T_F) (11 C_A - 4 n_f T_F)} \\
&- C_A (m_1^2 + m_2^2) \left(15 C_A^3 - 188 C_A^2 n_f T_F - 2 n_f^2 T_F^2 (27 C_F + 10 n_f T_F) + C_A n_f T_F (216 C_F \right. \\
&+ 137 n_f T_F) \left. \right) z^{\frac{8}{3}(2 C_A - n_f T_F)} \frac{1}{12 m_1 m_2 (11 C_A - 4 n_f T_F)^2 (2 C_A - n_f T_F)} \\
&- \frac{5 C_A^2 \left(1 - z^{\frac{1}{3}(5 C_A - 4 n_f T_F)} \right) \left(m_2^2 \ln \left(\frac{\nu_h}{m_1} \right) + m_1^2 \ln \left(\frac{\nu_h}{m_2} \right) \right)}{2 m_1 m_2 (5 C_A - 4 n_f T_F)} \left. \right]. \tag{65}
\end{aligned}$$

We do not aim in this paper to give a full fledged phenomenological analysis. Still, we

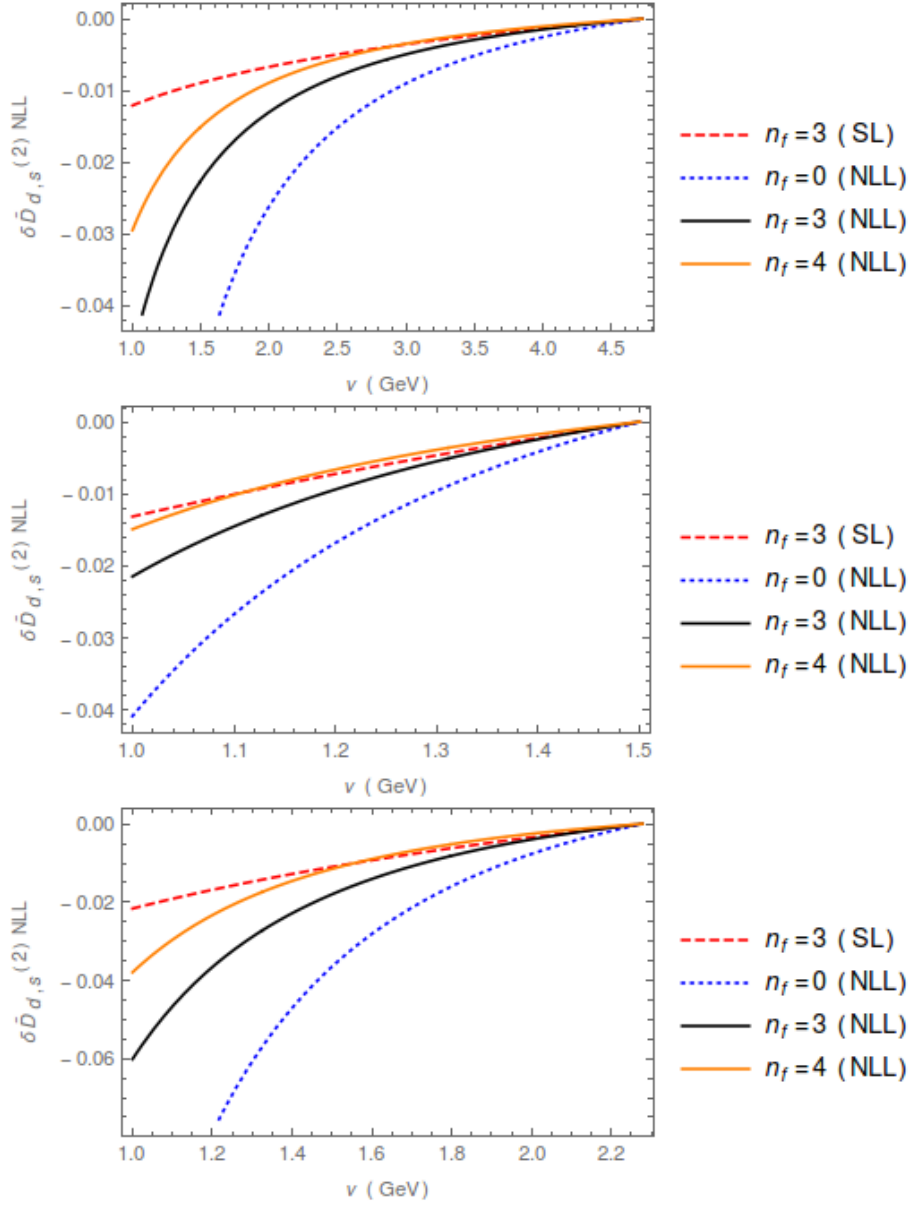


Figure 4: Plot of the NLL soft running due to Eq. (65) to $\delta \tilde{D}_{d,s}^{(2)NLL}$ for different values of n_f (0,3,4) and in the single log (SL) approximation (in this case only with $n_f = 3$). **Upper panel:** Plot for bottomonium with $\nu_h = m_b$. **Middle panel:** Plot for charmonium with $\nu_h = m_c$. **Lower panel:** Plot for B_c with $\nu_h = 2m_b m_c / (m_b + m_c)$.

compute numerically the running of $\delta \tilde{D}_{d,s}^{(2)NLL}$ to see its size. We show the result in Fig. 4. The contribution is small.

To this contribution one should also add the contributions generated by the new α^3/m^2 potentials that appear after using the full equations of motion. Of those we only

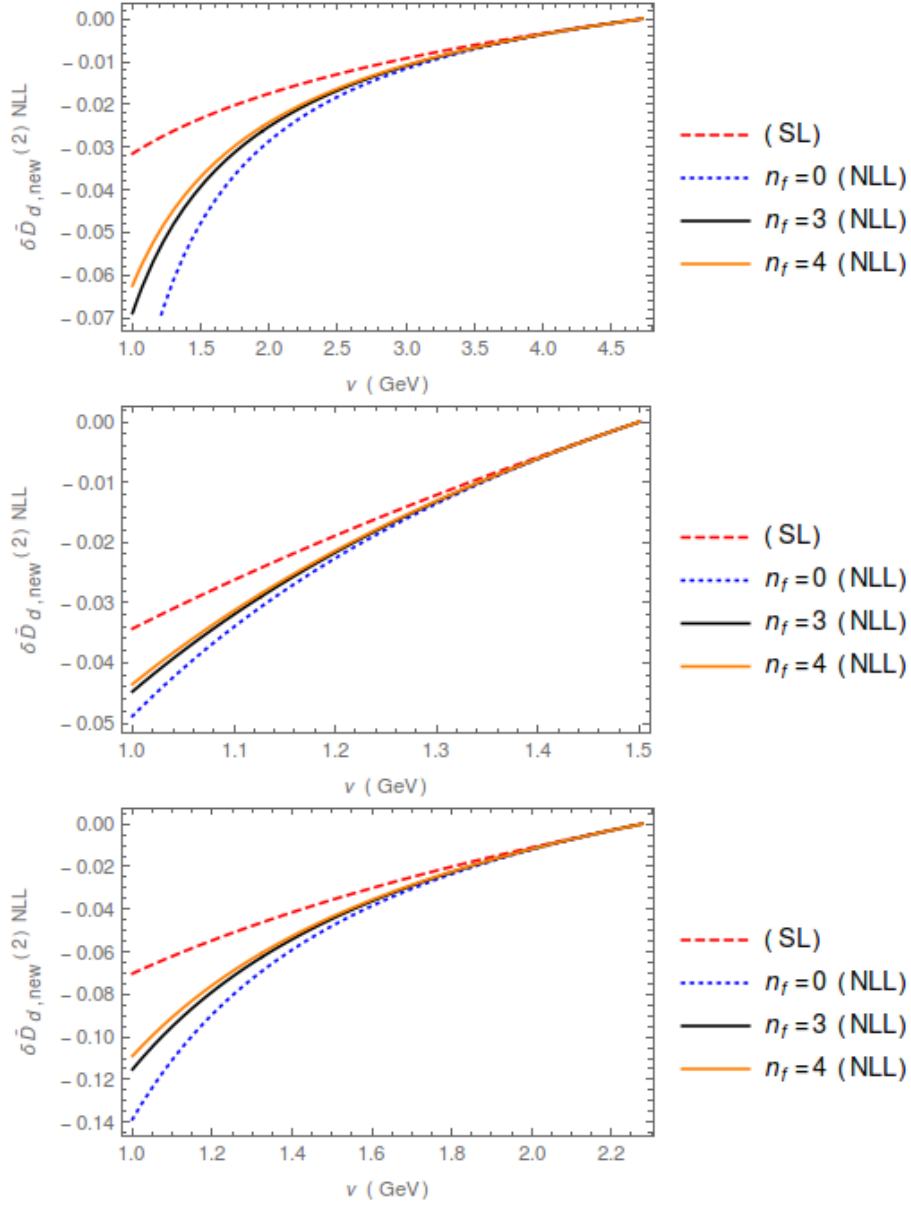


Figure 5: Plot of the extra contribution to the NLL soft running, $\delta \tilde{D}_{d,s}^{(2)NLL}$, due to Eq. (67), for different values of n_f (0,3,4) and in the single log (SL) approximation (in this case only with $n_f = 3$). **Upper panel:** Plot for bottomonium with $\nu_h = m_b$. **Middle panel:** Plot for charmonium with $\nu_h = m_c$. **Lower panel:** Plot for B_c with $\nu_h = 2m_b m_c / (m_b + m_c)$.

computed the contributions proportional to $c_F^{(i)2}$ and c_1^{hl} (the latter happened to be zero).

This generates a new contribution to the soft RG equation:

$$\nu_s \frac{d}{d\nu_s} (d_{ss} + C_F \bar{d}_{vs}) \Big|_{soft} = \dots + \frac{1}{16} C_F^2 C_A g^2 \alpha^2 \left[\frac{m_2}{m_1} c_F^{(1)2} + \frac{m_1}{m_2} c_F^{(2)2} \right]. \quad (66)$$

Its solution reads

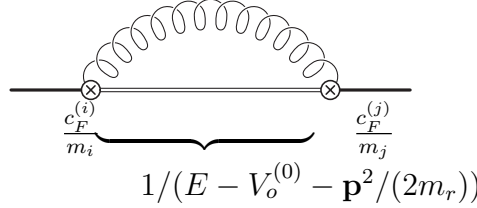
$$\delta \tilde{D}_{d,new}^{(2)NLL} = \frac{1}{\pi C_F} (d_{ss} + C_F \bar{d}_{vs}) = - \frac{\pi C_A C_F (m_1^2 + m_2^2) (1 - z^{-2(C_A - \beta_0)}) \alpha^2 (\nu_h)}{4m_1 m_2 (C_A - \beta_0)}. \quad (67)$$

We then show the size of this new contribution in Fig. 5.

Finally, let us note that the c_k^2 terms can also mix with α^2/m^3 potentials through field redefinitions, see the discussion in the Appendix. Therefore, this contribution could be different for other matching schemes.

5.2 Ultrasoft running

To obtain the complete potential RG equation, we also need an extra potential divergence that is generated by ultrasoft divergences. This term was already computed in [36], and applied to the spin-dependent case. Here, we give the full term, which contributes to both, the spin-dependent and spin-independent term. It is generated by the following diagram



which produces the following ultrasoft RG equation

$$\begin{aligned} \nu_{us} \frac{dV_{\mathbf{S}^2, 1/r^3}}{d\nu_{us}} &= \frac{4C_F}{3} \left[\frac{2\mathbf{S}_1 \cdot \mathbf{S}_2 c_F^{(1)}(\nu_{us}) c_F^{(2)}(\nu_{us})}{m_1 m_2} - \frac{3}{4} \left(\frac{c_F^{(1)2}(\nu_{us})}{m_1^2} + \frac{c_F^{(2)2}(\nu_{us})}{m_2^2} \right) \right] \\ &\times \left((V_o - V_s)^3 + \left(\frac{1}{m_1} + \frac{1}{m_2} \right) \frac{(V_o - V_s)^2}{2r^2} \right) \left[\frac{\alpha(\nu_{us})}{2\pi} \right], \end{aligned} \quad (68)$$

or alternatively (but equivalent at this order)

$$\begin{aligned} \nu_{us} \frac{dV_{\mathbf{S}^2, 1/r^3}}{d\nu_{us}} &= \frac{4C_F}{3} \left[\frac{2\mathbf{S}_1 \cdot \mathbf{S}_2 c_F^{(1)}(\nu_{us}) c_F^{(2)}(\nu_{us})}{m_1 m_2} - \frac{3}{4} \left(\frac{c_F^{(1)2}(\nu_{us})}{m_1^2} + \frac{c_F^{(2)2}(\nu_{us})}{m_2^2} \right) \right] \\ &\times V_o (V_o - V_s)^2 \left[\frac{\alpha(\nu_{us})}{2\pi} \right]. \end{aligned} \quad (69)$$

Using that the LL running of c_F is independent of the masses (we take the initial matching condition to be ν_h for both heavy quarks), its solution reads

$$V_{\mathbf{S}^2,1/r^3} = \frac{4C_F}{3} \left[\frac{2\mathbf{S}_1 \cdot \mathbf{S}_2}{m_1 m_2} - \frac{3}{4} \left(\frac{1}{m_1^2} + \frac{1}{m_2^2} \right) \right] V_o (V_o - V_s)^2 D_{1/r^3, \mathbf{S}^2}, \quad (70)$$

or

$$V_{\mathbf{S}^2,1/r^3} = \frac{4C_F}{3} \left[\frac{2\mathbf{S}_1 \cdot \mathbf{S}_2}{m_1 m_2} - \frac{3}{4} \left(\frac{1}{m_1^2} + \frac{1}{m_2^2} \right) \right] D_{1/r^3, \mathbf{S}^2} \times \left((V_o - V_s)^3 + \left(\frac{1}{m_1} + \frac{1}{m_2} \right) \frac{(V_o - V_s)^2}{2r^2} \right), \quad (71)$$

where (we use the same notation as in [36])

$$D_{1/r^3, \mathbf{S}^2} = \frac{1}{2C_A} \left[\left(\frac{\alpha(\nu_h)}{\alpha(\nu_{us})} \right)^{2C_A/\beta_0} - \left(\frac{\alpha(\nu_h)}{\alpha(1/r)} \right)^{2C_A/\beta_0} \right]. \quad (72)$$

$V_{\mathbf{S}^2,1/r^3}$ is singular and will contribute to the potential running of $\tilde{D}_d^{(2)}$.

5.3 Potential running

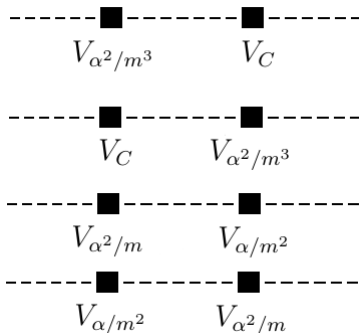


Figure 6: Divergent diagrams with one potential loop that contribute to the running of $\tilde{D}_d^{(2)}$ at $\mathcal{O}(\alpha^3)$.

We now have all the necessary preliminary ingredients to obtain the complete potential RG equation. The next step is to compute all potential loops that produce ultraviolet divergences that get absorbed in $\tilde{D}_d^{(2)}$ and are at most of $\mathcal{O}(\alpha^3)$. Since the delta-like potential is of $\mathcal{O}(1/m^2)$ we must construct potential loop diagrams of $\mathcal{O}(\alpha^n/m^2)$ with $n \leq 3$ describing the interaction between the two heavy quarks in the bound state through several potentials. The first non-vanishing contribution to the potential running is indeed of $\mathcal{O}(\alpha^3/m^2)$. To construct such potential loop diagrams, we must consider the power of α and m of each potential and take into account that each propagator adds an extra power

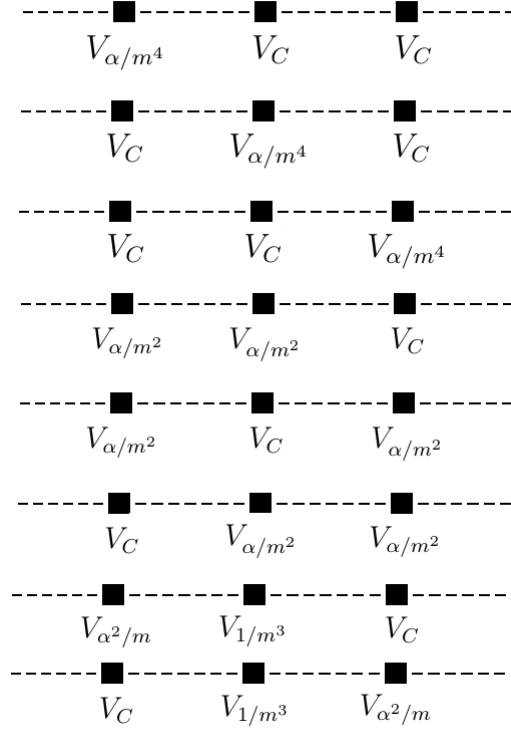


Figure 7: Divergent diagrams with two potential loops that contribute to the running of $\tilde{D}_d^{(2)}$ at $\mathcal{O}(\alpha^3)$.

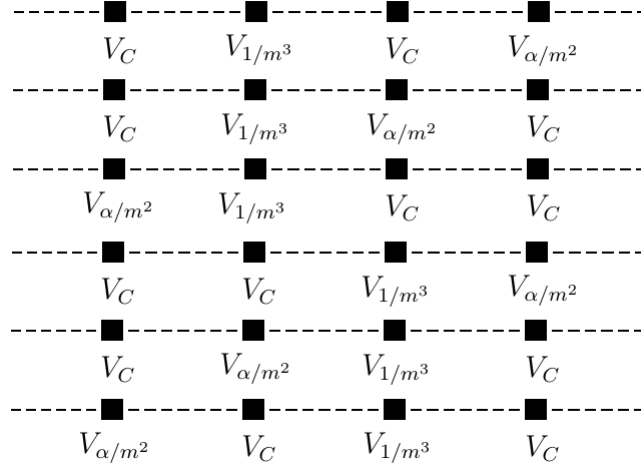


Figure 8: Divergent diagrams with three potential loops that contribute to the running of $\tilde{D}_d^{(2)}$ at $\mathcal{O}(\alpha^3)$.

of the mass m in the numerator. We summarize all kind of diagrams that contribute to the NLL potential running of $\tilde{D}_d^{(2)}$, in Figs. 6, 7, 8 and 9. The ultraviolet divergences

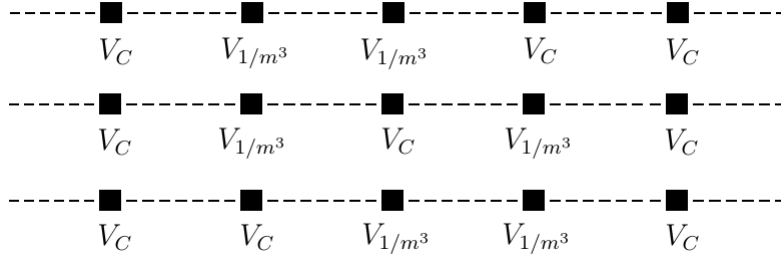


Figure 9: Divergent diagrams with four potential loops that contribute to the running of $\tilde{D}_d^{(2)}$ at $\mathcal{O}(\alpha^3)$.

arising in such diagrams must be absorbed in the $1/m^2$ potentials. However, after the computation, we observe that all divergences are only absorbed by the delta-like potential. It is important to mention that the iteration of two or more spin-dependent potentials can give a contribution to $\tilde{D}_d^{(2)}$, associated to a spin-independent potential. The relevant diagrams are shown in Figs. [6-9], where V_C is the tree level, $\mathcal{O}(\alpha)$, Coulomb potential, V_{α^r/m^s} is the $\mathcal{O}(\alpha^r/m^s)$ potential and V_{1/m^3} corresponds to the first relativistic correction to the kinetic energy, and it is proportional to c_4 .

It is interesting to discuss in more detail which, of the novel α^2/m^3 potentials computed in Secs. 4.2 and 4.4 (we remind that here we use the potentials after using the (free) equations of motion, i.e. the expressions in Sec. 4.4 for the energy dependent potentials), contribute to the running of $\tilde{D}_d^{(2)}$. The potentials in Eqs. (39-40) do not contribute to the running of $\tilde{D}_d^{(2)}$. Equation (39) does not because it is proportional to a total derivative, whereas Eq. (40) does not because of the following argument: the only possible potential loop that can be constructed with an $\mathcal{O}(\alpha^2/m^3)$ potential is the iteration of it with a Coulomb potential. As a consequence, the α^2/m^3 potential is always applied to an external momentum. When the high loop momentum limit is taken in the integral in order to find the ultraviolet pole, all these external momenta vanish and all the terms become proportional to $|\mathbf{k}|^{1+2\epsilon}$. After doing so and summing all the terms the overall coefficient is zero, explaining the fact that they do not contribute. This argument also applies to $\tilde{V}^{(e,1)}$ and $\tilde{V}^{(f,i)}$ (with $i = 1$ to 6). On the other hand $\tilde{V}^{(e,2)}$ and $\tilde{V}^{(f,7/8/9)}$ do contribute to the running. Note that $\tilde{V}^{(f,8)}$ and $\tilde{V}^{(f,9)}$ were originally dependent on the energy.

Diagrams with V_{1/m^3} in the extremes of a potential loop, i.e. acting over a external momentum have not been drawn because they do not produce any ultraviolet divergence. Similarly, diagrams with V_{1/m^5} do not produce ultraviolet divergences. One can then easily convince himself that there are no diagrams with five potential loops or more that can contribute to the $\mathcal{O}(\alpha^3)$ anomalous dimension of \tilde{D}_d . Therefore, the above discussion exhausts all possible contributions to the $\mathcal{O}(\alpha^3)$ anomalous dimension of \tilde{D}_d , and the

potential RG equation finally reads

$$\begin{aligned}
\nu \frac{d\tilde{D}_d^{(2)}}{d\nu} &= -2C_F^2 \alpha_V^2 m_r^3 \left(\frac{c_4^{(1)}}{m_1^3} + \frac{c_4^{(2)}}{m_2^3} \right) D_d^{(2)} \\
&+ C_F^2 \alpha_V \frac{m_r^2}{m_1 m_2} \left(D_d^{(2)2} - 8D_d^{(2)} D_1^{(2)} + 12D_1^{(2)2} - \frac{5}{6} D_{S_{12}}^{(2)2} + \frac{4}{3} D_{S^2}^{(2)2} \right) \\
&+ 2C_F^2 \alpha_V^2 m_r^3 \left(\frac{c_4^{(1)}}{m_1^3} + \frac{c_4^{(2)}}{m_2^3} \right) \left(4D_1^{(2)} \right) \\
&+ C_F C_A \left[2D_1^{(2)} D^{(1)} - D_d^{(2)} D^{(1)} + D^{(1)} \alpha_V m_r m_1 m_2 \left(\frac{c_4^{(1)}}{m_1^3} + \frac{c_4^{(2)}}{m_2^3} \right) \right] \\
&+ C_F^2 \alpha_V^3 m_r^4 m_1 m_2 \left(\frac{c_4^{(1)}}{m_1^3} + \frac{c_4^{(2)}}{m_2^3} \right)^2 \\
&+ \left(\frac{m_1}{m_2} + \frac{m_2}{m_1} \right) \frac{C_A^2 (C_A - 2C_F) \alpha_s^3}{2} D_{S^2, 1/r^3}^{(2)} \\
&- 2C_F^2 \alpha_V^2 \alpha m_r^2 \left[16m_1 m_2 \left(\frac{c_{X1}^{(1)}}{m_1^4} + \frac{c_{X1}^{(2)}}{m_2^4} \right) + 2 \left(\frac{c_4^{(1)}}{m_1^2} + \frac{c_4^{(2)}}{m_2^2} \right) + \frac{1}{m_1 m_2} + \left(\frac{c_M^{(1)}}{m_1^2} + \frac{c_M^{(2)}}{m_2^2} \right) \right] \\
&+ C_F \left(2C_F - \frac{C_A}{2} \right) \alpha^2 \alpha_V m_r m_1 m_2 \left[\frac{1}{2} \left(\frac{c_{A1}^{(1)}}{m_1^3} + \frac{c_{A1}^{(2)}}{m_2^3} \right) + \frac{1}{4} \left(\frac{c_{A2}^{(1)}}{m_1^3} + \frac{c_{A2}^{(2)}}{m_2^3} \right) + \frac{1}{m_1 m_2} \left(\frac{c_F^{(1)2}}{m_1} + \frac{c_F^{(2)2}}{m_2} \right) \right] \\
&- \frac{1}{2} C_F C_A \alpha^2 \alpha_V m_r m_1 m_2 \left[2 \left(\frac{c_4^{(1)}}{m_1^3} + \frac{c_4^{(2)}}{m_2^3} \right) + \left(\frac{1}{m_1^3} + \frac{1}{m_2^3} \right) - \left(\frac{c_M^{(1)}}{m_1^3} + \frac{c_M^{(2)}}{m_2^3} \right) + \left(\frac{c_F^{(1)2}}{m_1^3} + \frac{c_F^{(2)2}}{m_2^3} \right) \right. \\
&\left. - \left(\frac{c_F^{(1)} c_S^{(1)}}{m_1^3} + \frac{c_F^{(2)} c_S^{(2)}}{m_2^3} \right) \right] + \frac{T_F}{N_c} C_F \alpha^2 \alpha_V m_r m_1 m_2 \left[\left(\frac{c_{A3}^{(1)}}{m_1^3} + \frac{c_{A3}^{(2)}}{m_2^3} \right) + \frac{1}{2} \left(\frac{c_{A4}^{(1)}}{m_1^3} + \frac{c_{A4}^{(2)}}{m_2^3} \right) \right].
\end{aligned} \tag{73}$$

The first five lines are generated by potential loops with α^2/m , α/m^2 and the \mathbf{p}^4/m^3 correction to the kinetic energy (besides the iteration of the Coulomb potential, accounted for by α_V). The 6th line is the term generated by the potential computed in Sec. 5.2. The last four lines are generated by potential loops with the α^2/m^3 and α/m^4 potentials (besides the iteration of the Coulomb potential, accounted for by α_V). Note that, for simplicity, we have already used $c_k^{(i)} = 1$ [39] in the terms that do not have NRQCD Wilson coefficients in the above expression. A part of this equation was already computed in [40]. Also, several of these terms (for QED) can be checked with the computations in [34].

It is interesting to see that there is a matching scheme dependence of the individual α^2/m^3 and α/m^4 potentials that cancels out in the sum. In the above expression the coefficients c_{A2} , c_D , c_M , c_{X1} appear (note that the last two coefficients are dependent on c_D due to reparameterization invariance). They are gauge dependent quantities. Such

gauge dependence should vanish in the final result. Indeed it does. This is actually a strong check of the computation. In Eq. (73) we can approximate $\alpha_V = \alpha$ (everything is needed with LL accuracy). Then we can show that everything can be written in terms of \bar{c}_{A_2} , which is gauge independent (it is an observable in the low energy limit of the Compton scattering, see the discussion in [14]), and the explicit dependence in c_D , c_M , c_{X_1} , c_{A_2} disappears. The resulting expression reads

$$\begin{aligned}
\nu \frac{d\tilde{D}_d^{(2)}}{d\nu} &= -2c_4 C_F^2 \alpha_V^2 m_r^3 \left(\frac{1}{m_1^3} + \frac{1}{m_2^3} \right) D_d^{(2)} \tag{74} \\
&+ C_F^2 \alpha_{V_s} \frac{m_r^2}{m_1 m_2} \left(D_d^{(2)2} - 8D_d^{(2)} D_1^{(2)} + 12D_1^{(2)2} - \frac{5}{6} D_{S_{12}}^{(2)2} + \frac{4}{3} D_{S^2}^{(2)2} \right) \\
&+ 2c_4 C_F^2 \alpha_V^2 m_r^3 \left(\frac{1}{m_1^3} + \frac{1}{m_2^3} \right) (4D_1^{(2)}) \\
&+ C_F C_A \left[2D_1^{(2)} D^{(1)} - D_d^{(2)} D^{(1)} + c_4 D^{(1)} \alpha_V m_r m_1 m_2 \left(\frac{1}{m_1^3} + \frac{1}{m_2^3} \right) \right] \\
&+ c_4^2 C_F^2 \alpha_V^3 m_r^4 m_1 m_2 \left(\frac{1}{m_1^3} + \frac{1}{m_2^3} \right)^2 \\
&+ \left(\frac{m_1}{m_2} + \frac{m_2}{m_1} \right) \frac{C_A^2 (C_A - 2C_F) \alpha^3}{2} D_{S^2, 1/r^3}^{(2)} \\
&- 2C_F^2 \alpha^3 m_r^2 \left[\frac{5}{8} m_1 m_2 \left(\frac{1}{m_1^4} + \frac{1}{m_2^4} \right) + 2 \left(\frac{c_4^{(1)}}{m_1^2} + \frac{c_4^{(2)}}{m_2^2} \right) + \frac{1}{m_1 m_2} \right] \\
&+ C_F \left(2C_F - \frac{C_A}{2} \right) \alpha^3 m_r m_1 m_2 \left[\frac{1}{2} \left(\frac{c_{A1}^{(1)}}{m_1^3} + \frac{c_{A1}^{(2)}}{m_2^3} \right) + \frac{1}{4} \left(\frac{\bar{c}_{A2}^{(1)}}{m_1^3} + \frac{\bar{c}_{A2}^{(2)}}{m_2^3} \right) + \frac{1}{m_1 m_2} \left(\frac{c_F^{(1)2}}{m_1} + \frac{c_F^{(2)2}}{m_2} \right) \right] \\
&- \frac{1}{2} C_F C_A \alpha^3 m_r m_1 m_2 \left[2 \left(\frac{c_4^{(1)}}{m_1^3} + \frac{c_4^{(2)}}{m_2^3} \right) + \left(\frac{1}{m_1^3} + \frac{1}{m_2^3} \right) + \left(\frac{c_F^{(1)2}}{m_1^3} + \frac{c_F^{(2)2}}{m_2^3} \right) \right. \\
&\left. - \left(\frac{c_F^{(1)} c_S^{(1)}}{m_1^3} + \frac{c_F^{(2)} c_S^{(2)}}{m_2^3} \right) \right] - \left(C_F - \frac{C_A}{2} \right) C_F \alpha^3 m_r m_1 m_2 \left[\left(\frac{c_{A3}^{(1)}}{m_1^3} + \frac{c_{A3}^{(2)}}{m_2^3} \right) + \frac{1}{2} \left(\frac{c_{A4}^{(1)}}{m_1^3} + \frac{c_{A4}^{(2)}}{m_2^3} \right) \right].
\end{aligned}$$

From this result one may think that c_{A_3} and c_{A_4} contribute to the Abelian case. Nevertheless, the LO matching condition is zero for these Wilson coefficients, and all the running vanishes in the Abelian limit. Therefore, there is no contradiction with the pure QED case.

In order to solve Eq. (74), we need to introduce the D 's, the Wilson coefficients of the potentials. The necessary expressions can be found in Sec. 3. Note that in those expressions we have already correlated the ultrasoft factorization scale ν_{us} with ν and ν_h using $\nu_{us} = \nu^2/\nu_h$. We also do so in Eq. (72) (where we also set $1/r = \nu$, consistent with the precision of our computation). This correlation of scales was first introduced and motivated in [41].

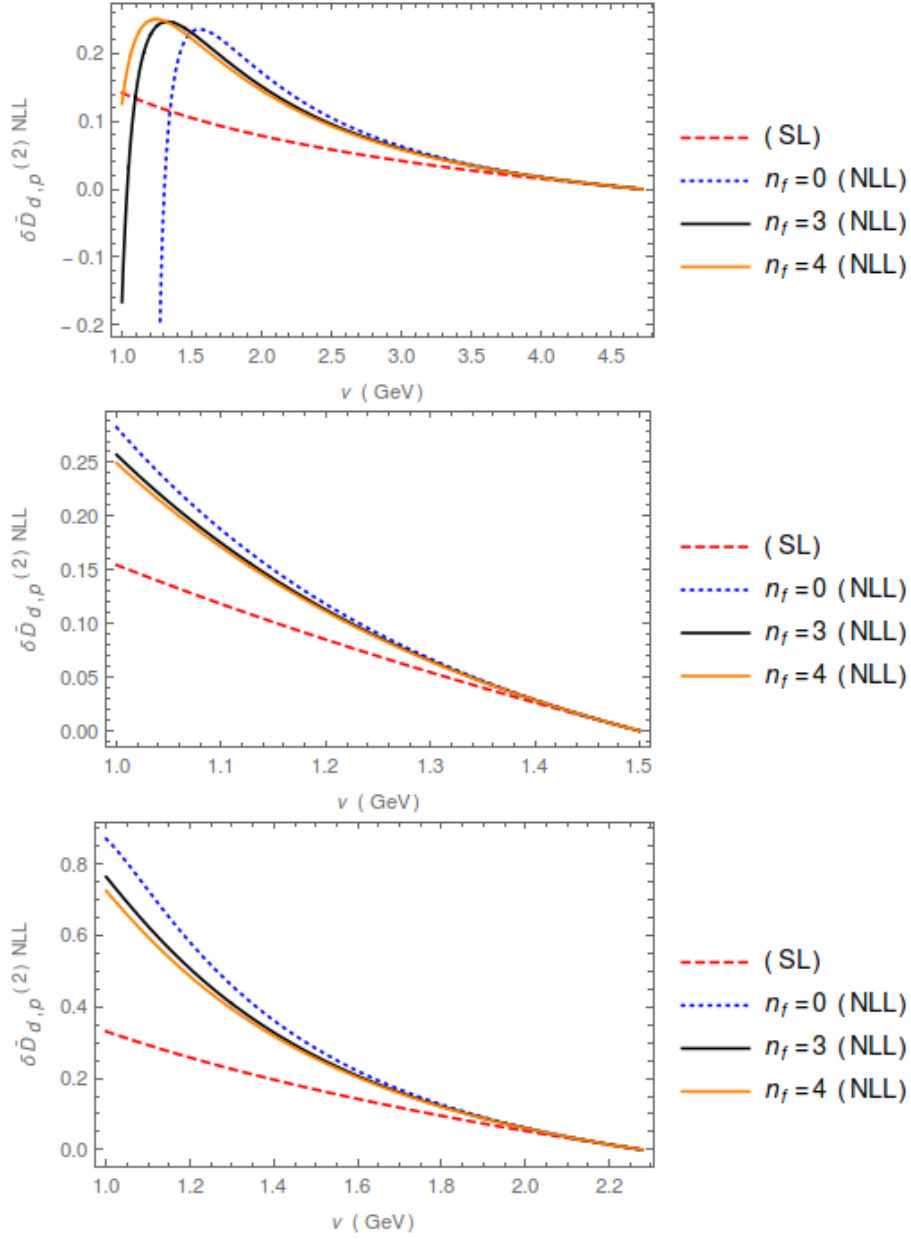


Figure 10: Plot of $\delta \tilde{D}_{d,p}^{(2)NLL}$ for different values of n_f (0,3,4) and in the single log (SL) approximation (in this case only with $n_f = 3$). **Upper panel:** Plot for bottomonium with $\nu_h = m_b$. **Middle panel:** Plot for charmonium with $\nu_h = m_c$. **Lower panel:** Plot for B_c with $\nu_h = 2m_b m_c / (m_b + m_c)$.

For $n_f = 3$ or 4 it is not possible to get an analytic result for the solution of the RG equation, more specifically for the coefficients multiplying the different z functions (note that this comes back to the fact that the polarizability Wilson coefficients c_{A1} , c_{A2} , ..., cannot be computed analytically). On top of that the resulting expressions are too long.

Therefore, we only explicitly show the analytic result with $n_f = 0$. It reads

$$\begin{aligned}
\delta\tilde{D}_{d,p}^{(2)NLL} = & \pi\alpha(\nu_h)^2 \left[-\frac{1}{48656036000C_A^3m_1^5m_2^5} \left(4561503375C_A^4m_1^4m_2^4(m_1^2 + m_2^2) \right. \right. \\
& -1754688000C_F^4m_1^2m_2^2(18m_1^4 + 142m_1^3m_2 + 101m_1^2m_2^2 + 142m_1m_2^3 + 18m_2^4)m_r^2 \\
& -14250C_A^3C_Fm_1^3m_2^3(480m_1^3(1924m_2 - 5885m_r) + 481m_1^2m_2(720m_2 - 1331m_r) \\
& +481m_1m_2^2(1920m_2 - 1331m_r) - 2824800m_2^3m_r) - 98800C_AC_F^3m_1m_2 \left(-293040m_2^5m_r^3 \right. \\
& -222m_1m_2^4m_r^2(691m_2 + 5720m_r) + m_1^2m_2^3m_r(-144320m_2^2 + 2370183m_2m_r - 293040m_r^2) \\
& +2m_1^5(497280m_2^3 - 72160m_2^2m_r - 76701m_2m_r^2 - 146520m_r^3) + 111m_1^4m_2(15680m_2^3 \\
& +21353m_2m_r^2 - 11440m_r^3) + 444m_1^3m_2^2(2240m_2^3 - 1831m_2m_r^2 - 660m_r^3) \left. \right) \\
& -4C_A^2C_F^2 \left(-2741700m_1^2m_2^5(5109m_2 - 1100m_r)m_r^2 - 5767851375m_1m_2^6m_r^3 \right. \\
& +3317457000m_2^6m_r^4 - 25m_1^3m_2^3m_r(298447930m_2^3 + 693732351m_2^2m_r + 230714055m_2m_r^2 \\
& -265396560m_r^3) + 27417m_1^4m_2^3(380000m_2^3 + 332750m_2^2m_r - 922808m_2m_r^2 - 210375m_r^3) \\
& +685425m_1^5m_2^2(9440m_2^3 + 13310m_2^2m_r - 25303m_2m_r^2 + 4400m_r^3) \\
& +25m_1^6(416738400m_2^4 - 298447930m_2^3m_r - 560293812m_2^2m_r^2 - 230714055m_2m_r^3 \\
& \left. +132698280m_r^4) \right) \left. \right) + \frac{1}{1375C_A^2m_1^3m_2^3} \left(6C_F^2 \left(100C_F(2m_1^4 - 3m_1^3m_2 + 4m_1^2m_2^2 - 3m_1m_2^3 \right. \right. \\
& \left. \left. +2m_2^4) + C_A(200m_1^4 + 75m_1^3m_2 + 334m_1^2m_2^2 + 75m_1m_2^3 + 200m_2^4) \right) m_r^2 z^{5C_A/3} \right) \\
& - \frac{3C_F^2(25m_1^4 - 32m_1^2m_2^2 + 25m_2^4)m_r^2 z^{10C_A/3}}{500C_Am_1^3m_2^3} \\
& + \frac{24C_F(43C_A^2 - 66C_AC_F - 40C_F^2)(m_1^3 + m_2^3)m_r z^{11C_A/3}}{605C_A^2m_1^2m_2^2} \\
& - \frac{1}{1331C_A^3m_1^4m_2^4} 6C_F \left(32C_F^3m_1m_2(2m_1^4 + 36m_1^3m_2 + 19m_1^2m_2^2 + 36m_1m_2^3 + 2m_2^4)m_r^2 \right. \\
& +11C_A^3m_1^2m_2^2 \left(3m_1^2m_2^2 + 8m_1m_2^3 + 8m_1^3(m_2 - m_r) - 8m_2^3m_r \right) + 8C_AC_F^2m_1m_2 \left(132m_1m_2^3m_r^2 \right. \\
& -m_2^3m_r^2(8m_2 + 77m_r) + 8m_1^4(6m_2^2 - m_r^2) + 8m_1^2(6m_2^4 - 7m_2^2m_r^2) + m_1^3(96m_2^3 + 132m_2m_r^2 \\
& -77m_r^3) \left. \right) + 2C_A^2C_F \left(44m_2^5m_r^3 - m_1m_2^4m_r^2(64m_2 + 55m_r) + 4m_1^2m_2^3m_r(-22m_2^2 + 32m_2m_r \right. \\
& +11m_r^2) + m_1^4m_2(38m_2^3 + 128m_2m_r^2 - 55m_r^3) + m_1^3m_2^2(96m_2^3 - 71m_2m_r^2 + 44m_r^3) \\
& \left. \left. +m_1^5(96m_2^3 - 88m_2^2m_r - 64m_2m_r^2 + 44m_r^3) \right) \right) z^{11C_A/3} \\
& - \frac{99(3C_A - 8C_F)C_F(m_1^3 + m_2^3)m_r z^{13C_A/3}}{442C_Am_1^2m_2^2} + \frac{(C_A - 2C_F)C_F(m_1^3 + m_2^3)m_r z^{16C_A/3}}{10C_Am_1^2m_2^2} \\
& + \frac{(C_A - 4C_F)C_F(11m_1^3 + 3m_1^2m_2 + 3m_1m_2^2 + 11m_2^3)m_r z^{16C_A/3}}{16C_Am_1^2m_2^2}
\end{aligned}$$

$$\begin{aligned}
& + \frac{1}{352C_A^2 m_1^4 m_2^4} 3 \left(11C_A^3 m_1^3 m_2^3 (m_1^2 + m_2^2) - 22C_A^2 C_F m_1^2 m_2^2 (m_1^3 + m_2^3) m_r - 16C_F^3 m_1 m_2 (2m_1^4 \right. \\
& - 3m_1^3 m_2 + 4m_1^2 m_2^2 - 3m_1 m_2^3 + 2m_2^4) m_r^2 - 4C_A C_F^2 (m_1^2 + m_2^2) m_r^2 \left(-19m_1^2 m_2^2 + 8m_1 m_2^3 \right. \\
& \left. \left. + m_1^3 (8m_2 - 11m_r) - 11m_2^3 m_r \right) \right) z^{16C_A/3} + \frac{6C_F^2 (m_1^3 + m_2^3) m_r z^{19C_A/3}}{19C_A m_1^2 m_2^2} \\
& + \frac{3C_F (51C_A^2 - 54C_A C_F - 224C_F^2) (m_1^3 + m_2^3) m_r z^{22C_A/3}}{121C_A^2 m_1^2 m_2^2} \\
& + \frac{1}{5324C_A^3 m_1^5 m_2^5} 3C_F \left(-64C_F^3 m_1^2 m_2^2 (10m_1^4 - 2m_1^3 m_2 + 25m_1^2 m_2^2 - 2m_1 m_2^3 + 10m_2^4) m_r^2 \right. \\
& + 2C_A^3 m_1^3 m_2^3 \left(42m_1^2 m_2^2 + 112m_1 m_2^3 + 209m_2^3 m_r + m_1^3 (112m_2 - 209m_r) \right) \\
& - 32C_A C_F^2 m_1 m_2 \left(-33m_2^5 m_r^3 + m_1 m_2^4 m_r^2 (32m_2 + 11m_r) - m_1^2 m_2^3 m_r^2 (47m_2 + 33m_r) \right. \\
& + m_1^5 (16m_2^3 + 32m_2 m_r^2 - 33m_r^3) + m_1^3 m_2^2 (16m_2^3 + 87m_2 m_r^2 - 33m_r^3) \\
& + m_1^4 m_2 (4m_2^3 - 47m_2 m_r^2 + 11m_r^3) \left. \right) + C_A^2 C_F \left(m_1^2 m_2^5 (221m_2 - 1320m_r) m_r^2 + 880m_1 m_2^6 m_r^3 \right. \\
& - 484m_2^6 m_r^4 + 8m_1^3 m_2^3 m_r (44m_2^3 + 356m_2^2 m_r + 110m_2 m_r^2 - 121m_r^3) - 8m_1^5 m_2^2 (42m_2^3 \\
& - 356m_2 m_r^2 + 165m_r^3) + 4m_1^4 m_2^3 (4m_2^3 + 149m_2 m_r^2 + 220m_r^3) + m_1^6 (16m_2^4 + 352m_2^3 m_r \\
& \left. + 221m_2^2 m_r^2 + 880m_2 m_r^3 - 484m_r^4) \right) z^{22C_A/3} - \frac{1}{11949113C_A^2 m_1^2 m_2^2} \left(4(3C_A - 10C_F) C_F \right. \\
& \times \left((2691765 + 51647\sqrt{157}) C_A + 272(10205 - 269\sqrt{157}) C_F \right) (m_1^3 + m_2^3) m_r z^{-\frac{1}{12}(-71+\sqrt{157})C_A} \left. \right) \\
& + \frac{1}{11949113C_A^2 m_1^2 m_2^2} \left(4(3C_A - 10C_F) C_F \left((-2691765 + 51647\sqrt{157}) C_A - 272(10205 \right. \right. \\
& \left. \left. + 269\sqrt{157}) C_F \right) (m_1^3 + m_2^3) m_r z^{\frac{1}{12}(71+\sqrt{157})C_A} \right) \\
& + \frac{1}{32m_1 m_2} \left(3(C_A - 2C_F) (m_1^2 + m_2^2) \text{Hypergeometric2F1}(-6/11, 1, 27/11, -1) \right) \\
& - \frac{1}{16 \cdot 2^{5/11} m_1 m_2 (2 - z^{11C_A/3})^{6/11}} \left(3(C_A - 2C_F) (m_1^2 + m_2^2) z^{22C_A/3} (-1 + 2z^{-11C_A/3})^{6/11} \right. \\
& \times \text{Hypergeometric2F1}(-6/11, 16/11, 27/11, z^{11C_A/3}/2) \left. \right) - \frac{1}{18C_A^2 m_1^3 m_2^3} \left(C_F (m_1^2 + m_2^2) \right. \\
& \times \left(C_A^2 m_1^2 m_2^2 + 2C_F^2 (m_1 + m_2)^2 m_r^2 + C_A C_F (2m_1 m_2 m_r^2 + m_2^2 m_r^2 + m_1^2 (2m_2^2 + m_r^2)) \right) \\
& \times \text{Hypergeometric2F1}(1, 1, 38/11, -1) \left. \right) + \frac{1}{36C_A^2 m_1^3 m_2^3} \left(C_F (C_A + 2C_F) (m_1^2 + m_2^2) \right. \\
& \times \left(C_A m_1^2 m_2^2 + C_F (m_1 + m_2)^2 m_r^2 \right) z^{9C_A} \text{Hypergeometric2F1}(1, 27/11, 38/11, z^{11C_A/3}/2) \left. \right)
\end{aligned}$$

$$\begin{aligned}
& -\frac{1}{3025C_A^2m_1^3m_2^3}8C_F^2\left(100C_F^2(2m_1^2-3m_1m_2+2m_2^2)^2+50C_AC_F(16m_1^4-18m_1^3m_2\right. \\
& +23m_1^2m_2^2-18m_1m_2^3+16m_2^4)+C_A^2(400m_1^4+300m_1^3m_2+1673m_1^2m_2^2+300m_1m_2^3 \\
& \left.+400m_2^4)\right)m_r^2\ln(z)-\frac{1}{1331C_A^3m_1^4m_2^4}96C_F(m_1+m_2)\left(-11C_A^3m_1^2m_2^2(m_1^2-m_1m_2\right. \\
& +m_2^2)m_r+24C_F^3m_1m_2(m_1+m_2)^3m_r^2+2C_AC_F^2(m_1+m_2)\left(2m_1^2m_2^2m_r^2+12m_1m_2^3m_r^2\right. \\
& -11m_2^3m_r^3+m_1^3(24m_2^3+12m_2m_r^2-11m_r^3)\left)+C_A^2C_F\left(-22m_1^2m_2^4m_r-11m_1m_2^3m_r^3\right. \\
& -11m_2^4m_r^3+m_1^4(13m_2^3-22m_2^2m_r-11m_r^3)+m_1^3(13m_2^4+22m_2^3m_r\right. \\
& \left.-11m_2m_r^3)\right)\ln(2-z^{11C_A/3})-\frac{1}{1331C_A^3m_1^3m_2^3}48C_F\left(C_A^3m_1^2m_2^2(8m_1^2+3m_1m_2+8m_2^2)\right. \\
& -56C_F^3m_1m_2(m_1+m_2)^2m_r^2+C_A^2C_F\left(19m_1m_2^3m_r^2+8m_2^4m_r^2+19m_1^3m_2(-2m_2^2+m_r^2)\right. \\
& +8m_1^4(m_2^2+m_r^2)+m_1^2(8m_2^4+22m_2^2m_r^2)\left)-2C_AC_F^2\left(11m_1m_2^3m_r^2-4m_2^4m_r^2+m_1^4(8m_2^2\right. \\
& \left.-4m_r^2)+11m_1^3m_2(4m_2^2+m_r^2)+m_1^2(8m_2^4+30m_2^2m_r^2)\right)\right)z^{11C_A/3}\ln(2-z^{11C_A/3}) \\
& +\frac{1}{22C_A^2m_1^3m_2^3}\left(3C_F(C_A+2C_F)(m_1^2+m_2^2)\left(C_Am_1^2m_2^2+C_F(m_1+m_2)^2m_r^2\right)z^{16C_A/3}\right. \\
& \left.\times\ln(2-z^{11C_A/3})\right)+\frac{24C_F}{1331C_A^3m_1^4m_2^4}\left(8C_F^3m_1m_2(m_1+m_2)^2(3m_1^2-m_1m_2+3m_2^2)m_r^2\right. \\
& +C_A^3m_1^2m_2^2\left(3m_1^2m_2^2+8m_1m_2^3+m_1^3(8m_2-11m_r)-11m_2^3m_r\right)+2C_AC_F^2\left(2m_1m_2^4(8m_2\right. \\
& -11m_r)m_r^2+m_1^2m_2^3(15m_2-11m_r)m_r^2-11m_2^5m_r^3+m_1^4m_2(4m_2^3+15m_2m_r^2-22m_r^3) \\
& +m_1^3m_2^2(16m_2^3-2m_2m_r^2-11m_r^3)+m_1^5(16m_2^3+16m_2m_r^2-11m_r^3)\left)+C_A^2C_F\left(2m_1m_2^4(4m_2\right. \\
& -11m_r)m_r^2-11m_2^5m_r^3+m_1^2m_2^3m_r(-22m_2^2+19m_2m_r-11m_r^2)+m_1^4m_2(-12m_2^3+19m_2m_r^2 \\
& -22m_r^3)+m_1^5(21m_2^3-22m_2^2m_r+8m_2m_r^2-11m_r^3)+m_1^3m_2^2(21m_2^3+22m_2m_r^2-11m_r^3)\right)\left.\right) \\
& \times z^{22C_A/3}\ln(2-z^{11C_A/3})+\frac{1}{1331C_A^3m_1^3m_2^3}\left(768C_F^2(m_1+m_2)^2\left(C_A^2m_1^2m_2^2\right. \right. \\
& \left. +C_F^2(m_1+m_2)^2m_r^2+C_AC_F(2m_1m_2m_r^2+m_2^2m_r^2+m_1^2(2m_2^2+m_r^2))\right)\ln^2(2-z^{11C_A/3}) \\
& \left.-\frac{1}{1331C_A^3m_1^3m_2^3}\left(192C_F^2(m_1+m_2)^2\left(C_A^2m_1^2m_2^2+C_F^2(m_1+m_2)^2m_r^2+C_AC_F(2m_1m_2m_r^2\right. \right. \right. \\
& \left. \left. +m_2^2m_r^2+m_1^2(2m_2^2+m_r^2))\right)\times z^{22C_A/3}\ln^2(2-z^{11C_A/3})\right)\left.\right]. \tag{75}
\end{aligned}$$

Finally, in Fig. 10, we give the numerical evaluation $\delta\tilde{D}_{d,p}^{(2)NLL}$ for different values of

n_f . The contribution is sizable.

5.4 Potential running, spin-dependent delta potential

Even though not relevant for this paper, we profit to present the potential RG equation of $\tilde{D}_{S^2}^{(2)}$ in the basis we use in this paper, which is different from the basis used in [36]. The final solution is nevertheless the same.

$$\begin{aligned}
\frac{d\tilde{D}_{S^2}^{(2)}}{d\ln\nu} = & -2m_r^3 \left(\frac{1}{m_1^3} + \frac{1}{m_2^3} \right) C_F^2 \alpha_V^2 D_{S^2}^{(2)} + \frac{m_r^2}{m_1 m_2} C_F^2 \alpha_V \left(2D_d^{(2)} D_{S^2}^{(2)} \right. \\
& \left. - \frac{4}{3} \left(D_{S^2}^{(2)} \right)^2 - 8D_{S^2}^{(2)} D_1^{(2)} - \frac{5}{12} \left(D_{S_{12}}^{(2)} \right)^2 \right) - C_A C_F D^{(1)} D_{S^2}^{(2)} \\
& + \frac{1}{2} \alpha^3 C_F^2 m_r^2 \left(\frac{c_{pp'}^{(1)}}{m_1^2} c_F^{(2)} + c_F^{(1)} \frac{c_{pp'}^{(2)}}{m_2^2} \right) - 2\alpha^3 C_F^2 \frac{m_r^2}{m_1 m_2} c_F^{(1)} c_F^{(2)} \\
& - \frac{1}{4} \alpha^3 C_F^2 \frac{m_r^2}{m_1 m_2} c_S^{(1)} c_S^{(2)} - \alpha^3 C_F^2 m_r^2 \left(c_F^{(1)} \frac{c_S^{(2)}}{m_2^2} + \frac{c_S^{(1)}}{m_1^2} c_F^{(2)} \right) \\
& + \frac{1}{2} \alpha^3 C_F (4C_F - C_A) m_r \left(c_F^{(1)} \frac{c_S^{(2)}}{m_2} + \frac{c_S^{(1)}}{m_1} c_F^{(2)} \right) \\
& + \frac{1}{8} \alpha^3 C_F C_A m_r \left(c_F^{(1)} \frac{c_F^{(2)2}}{m_2} + \frac{c_F^{(1)2}}{m_1} c_F^{(2)} \right) - \frac{C_A^2 (C_A - 2C_F) \alpha^3}{2} D_{S^2, 1/r^3}^{(2)}. \quad (76)
\end{aligned}$$

This equation has slightly changed with respect to Eq. (36) in [36] because of the change in the basis of potentials. In particular the term proportional to $D_{S^2}^{(2)}$ changes to compensate the fact that $D_d^{(2)}$ is also different so that the result is the same.

6 N³LL heavy quarkonium mass

For the organization of the computation and presentation of the results we closely follow the notation of [7]. In particular we split the total RG improved potential in the following way:

$$V_s^{N^i LL}(\nu_h, \nu) = V_s^{N^i LO}(\nu) + \delta V_s^{N^i LL}(\nu_h, \nu), \quad (77)$$

where $V_s^{N^i LO}(\nu) \equiv V_s^{N^i LL}(\nu_h = \nu, \nu)$. We then split the total energy into the N³LO result and the new contribution associated to the resummation of logarithms. The S-wave spectrum at N³LO was obtained in Ref. [42] for the ground state, in Refs. [43, 44] for S-wave states, and in Refs. [45, 46] for general quantum numbers but for the equal mass case. The result for the nonequal mass case was obtained in Ref. [6].

From the RG improved potential one obtains the N^i LL shift in the energy levels

$$E_{N^iLL}(\nu_h, \nu) = E_{N^iLO}(\nu) + \delta E_{RG}(\nu_h, \nu) \Big|_{N^iLL}. \quad (78)$$

where the explicit expression for $E_{N^iLO}(\nu)$ can be found in Ref. [6], and in a different spin basis in Appendix B of [7].

The LO and NLO energy levels are unaffected by the RG improvement, i.e.

$$\delta E_{RG} \Big|_{LL} = \delta E_{RG} \Big|_{NLL} = 0. \quad (79)$$

We now determine the variations with respect to the NNLO and N^3 LO results. We are here interested in the corrections associated to the resummation of logarithms. In order to obtain the spectrum at NNLL and N^3 LL we need to add the following energy shift to the NNLO and N^3 LO spectrum:

$$\delta E_{RG} \Big|_{NNLL} = \langle nl | \delta V_s^{NNLL}(\nu_h, \nu) | nl \rangle, \quad (80)$$

which was computed in Ref. [8], and

$$\delta E_{nl, RG} \Big|_{N^3LL} = \langle nl | \delta V_s^{N^3LL}(\nu_h, \nu) | nl \rangle \quad (81)$$

$$+ 2 \langle nl | V_1 \frac{1}{(E_n^C - h)'} \delta V_s^{NNLL}(\nu_h, \nu) | nl \rangle + [\delta E_{US}(\nu, \nu_{us}) - \delta E_{US}(\nu, \nu)] \quad (82)$$

Note that $\langle nl | \delta V_s^{N^3LL}(\nu_h, \nu) | nl \rangle$ includes $\langle nl | \delta V_s^{NNLL}(\nu_h, \nu) | nl \rangle$.

$\delta E_{nl, RG} \Big|_{N^3LL}$ was computed for $l \neq 0$ in Ref. [7], and for $l = 0$, $s = 1$ in Refs. [9, 10]. To have the complete result for S-wave states, one needs to compute (and add) the new term for $l = 0$

$$\delta E_{n0, RG}^{\text{new}} \Big|_{N^3LL} = \langle n0 | [\delta V_r^{N^3LL} - \delta V_r^{NNLL}] (\nu_h, \nu) | n0 \rangle + 2 \langle n0 | V_1 \frac{1}{(E_n^C - h)'} \delta V_r^{NNLL}(\nu_h, \nu) | n0 \rangle, \quad (83)$$

where

$$V_1 = -\frac{C_F \alpha}{r} \frac{\alpha}{4\pi} (2\beta_0 \ln(\nu r e^{\gamma_E}) + a_1), \quad (84)$$

and $\delta V_r^{N^iLL}$ is the delta-related potential contribution to $\delta V_s^{N^iLL}$. The new term generated

from $\tilde{D}_d^{(2)}$ then reads

$$\begin{aligned}
\delta E_{nl,\text{RG}}^{\text{new}} \Big|_{\text{N}^3\text{LL}} &= \frac{1}{m_1 m_2} \pi C_F [\delta \tilde{D}_d^{(2)NLL}(\nu_h, \nu) - \delta \tilde{D}_d^{(2)NLL}(\nu, \nu)] \frac{(m_r C_F \alpha)^3}{\pi n^3} \delta_{l0} \\
&+ 2 \frac{1}{m_1 m_2} \pi C_F [\tilde{D}_d^{(2)LL}(\nu_h, \nu) - \tilde{D}_d^{(2)LL}(\nu, \nu)] \left[-\frac{\alpha}{4\pi} \right] \frac{(m_r C_F \alpha)^3}{\pi n^3} \delta_{l0} \\
&\times \left\{ 2\beta_0 \left[\frac{1}{2} + \frac{\pi^2 n}{6} - n \Sigma_2^{(k)}(n, 0) - \frac{3}{2} \ln \left(\frac{n a \nu}{2} \right) - \frac{3}{2} S_1(n) \right] - \frac{3}{2} a_1 \right\} \\
&+ \frac{\pi C_F}{m_1 m_2} \left[-\frac{1}{4\pi} \right] \frac{2(m_r C_F \alpha)^3}{n^3} \left(\ln \frac{n a \nu}{2} - S_1(n) - \frac{n-1}{2n} \right) 2\delta_{l0} \\
&\times \left[\left(k \frac{d}{dk} \tilde{D}_d^{(2)} \right) \Big|_{k=\nu}^{LL} (\nu_h; \nu) - \left(k \frac{d}{dk} \tilde{D}_d^{(2)} \right) \Big|_{k=\nu}^{LL} (\nu; \nu) \right], \tag{85}
\end{aligned}$$

where $\delta \tilde{D}_d^{(2)NLL}$ is defined in Eq. (35). The first three lines are generated by the term proportional to $\delta^{(3)}(\mathbf{r})$. The last two lines are the contribution to the S-wave energy ($l=0$) from the last term of Eq. (21) (the contribution to the P-wave energy, proportional to $1-\delta_{l0}$ term, is already included in Ref. [7]. Therefore, we do not include it in the expression above). To this contribution we have explicitly subtracted the fixed order contribution already included in the N³LO result.

By adding $\delta E_{nl,\text{RG}}^{\text{new}} \Big|_{\text{N}^3\text{LL}}$ to the results computed in these references⁵ one obtains the complete result.

7 Conclusions

In this paper we have computed the α/m^4 , and the α^2/m^3 , spin-independent potentials (in the Coulomb gauge), and an extra ultrasoft correction that contributes to the S-wave spin-average NNNLL spectrum. We have also obtained the potential RG equation of the delta potential with NLL accuracy (the first nonzero contribution). Combined with the previous results we solve this equation and obtain the complete (potential and ultrasoft) NLL running of the delta potential.

We have also computed the bare and renormalized (soft-) α^3/m^2 contribution to the spin-independent delta-like potential proportional to $[c_F^{(1)}]^2$, $[c_F^{(2)}]^2$, $\bar{c}_1^{(1)hl}$ and $\bar{c}_1^{(2)hl}$ and obtained (and solved) the RG equation.

Combining all these results with the results in [7] and Refs. [9, 10] allows us to obtain the S-wave mass with N³LL accuracy. The missing terms to obtain the full results are to have the NLL running of \bar{c}_1^{hl} (the associated missing term is of $\mathcal{O}(T_f n_f m \alpha^6 \ln \alpha)$ and

⁵Note though that one should change $2 = S(S+1)$ by $S(S+1) - 3/2$ in the result obtained in [9, 10] to account for the change of basis of operators to the one we use here. One should also change from the on-shell to the Coulomb basis of potentials in [7] (this is very easy to do, as the ultrasoft running is not affected by this transformation).

is expected to be quite small. Its computation will be carried out elsewhere), and a piece of the soft running of the delta potential. This computation will be performed in a separate paper. The magnitude of this contribution is estimated to be smaller compared with the potential running computed in this paper. It is also expected to be smaller than the complete running of the heavy quarkonium potential. Nevertheless, a detailed phenomenological analysis is postponed to future publications.

Finally, we remark that significant parts of the computations above are necessary building blocks for a future N⁴LO evaluation of the heavy quarkonium spectrum.

Acknowledgments

We thank discussions with A.A. Penin, C. Peset, M. Stahlhofen and M. Steinhauser. We also thank A.A. Penin for partial checks of the computations of this paper. This work was supported in part by the Spanish grants FPA2014-55613-P, FPA2017-86989-P and SEV-2016-0588 from the ministerio de Ciencia, Innovación y Universidades, and the grant 2017SGR1069 from the Generalitat de Catalunya.

A Matching scheme (in)dependence

The potentials obtained in Sec. 4 were computed in the Coulomb gauge. On the other hand, the potential RG equation obtained in Sec. 5 is generated by potential loops, which are independent of the gauge/matching scheme. The dependence on the matching scheme of Eq. (74) is implicitly generated by the Wilson coefficients used for the running, such as $D_d^{(2)}$ or $D^{(1)}$, and explicitly, since we put the explicit expressions for the $1/m^3$ and $1/m^4$ potentials obtained in the Coulomb gauge. This last point makes that Eq. (74) can only be used in the Coulomb gauge matching scheme, though with not much effort it could be written in terms of general structures of the $1/m^3$ and $1/m^4$ potentials that would make it also useful for a computation in a general matching scheme. Nevertheless, since we do not know the $1/m^3$ and $1/m^4$ potentials in other matching schemes, we refrain from doing so in this paper. Still it is worth to study how the differences between different matching schemes show up in the terms where the entire matching scheme dependence is encoded in the D 's (the first four lines in Eq. (74)). We do so in the following.

At $\mathcal{O}(m\alpha^4)$ the Coulomb and Feynman matching schemes produce the same potential but the on-shell scheme does not. At this order, the relation between the Wilson coefficients of the delta-like and the $1/m$ potentials in the off-shell Coulomb gauge (equal to the Feynman gauge at this order) and in the on-shell scheme are given by:

$$D_{d,CG}^{(2)} = D_{d,ON}^{(2)} + \alpha(\nu), \quad (86)$$

$$D_{CG}^{(1)} = D_{ON}^{(1)} + \alpha^2(\nu) \frac{2C_F}{C_A} \frac{m_r^2}{m_1 m_2}. \quad (87)$$

At the order we are working in this paper such differences produce the following difference between the RG equation for $\tilde{D}_d^{(2)}$ in the two schemes (for the first four lines in Eq. (74)):

$$\nu \frac{d}{d\nu} (\tilde{D}_{d,CG}^{(2)} - \tilde{D}_{d,ON}^{(2)}) = C_F^2 \frac{m_r^2}{m_1 m_2} \left(-4\alpha^2 D_1^{(2)} + \alpha^3 - \alpha \frac{C_A}{C_F} \frac{m_1 m_2}{m_r^2} D_{CG}^{(1)} \right), \quad (88)$$

which does not vanish. This difference can be understood through field redefinitions. The field redefinition that moves from the off-shell Coulomb to the on-shell scheme was already discussed in [47, 6]. In the second reference the discussion was focused on effects to the spectrum up to $\mathcal{O}(m\alpha^5)$. We now need to see (the logarithmically enhanced) differences of $\mathcal{O}(m\alpha^6)$. They can be traced back by using the following Hamiltonian in the Coulomb (Feynman) gauge:

$$h_{CG} = h^{(0)} + h_{CG}^{(2)}, \quad (89)$$

where $h^{(0)} \sim mv^2$ is the leading order Hamiltonian:

$$h^{(0)} = \frac{\mathbf{p}^2}{2m_r} + V^{(0)}(r), \quad (90)$$

and $h_{CG}^{(2)} \sim mv^4$ is the relativistic correction, with the explicit potentials:

$$\begin{aligned} h_{CG}^{(2)} = & -c_4 \frac{\mathbf{p}^4}{8m_1^3} - c_4 \frac{\mathbf{p}^4}{8m_2^3} - \frac{C_F C_A D^{(1)}}{4m_r r^2} \\ & - \frac{C_F D_1^{(2)}}{2m_1 m_2} \left\{ \frac{1}{r}, \mathbf{p}^2 \right\} + \frac{C_F D_2^{(2)}}{2m_1 m_2} \frac{1}{r^3} \mathbf{L}^2 + \frac{\pi C_F D_d^{(2)}}{m_1 m_2} \delta^{(3)}(\mathbf{r}) \\ & + \frac{8\pi C_F D_{S^2}^{(2)}}{3m_1 m_2} \mathbf{S}_1 \cdot \mathbf{S}_2 \delta^{(3)}(\mathbf{r}) + \frac{3C_F}{2m_1 m_2} \frac{1}{r^3} \mathbf{L} \cdot (D_{LS_1}^{(2)} \mathbf{S}_1 + D_{LS_2}^{(2)} \mathbf{S}_2) + \frac{C_F D_{S_{12}}^{(2)}}{4m_1 m_2} \frac{1}{r^3} S_{12}(\hat{\mathbf{r}}). \end{aligned} \quad (91)$$

h_{CG} correctly reproduces the $\mathcal{O}(m\alpha^4)$ spectrum (for the purpose of the comparison we can neglect the $\mathcal{O}(\alpha)$ corrections to the static potential: $C_F \frac{\alpha v_s}{r} \simeq -C_F \alpha \frac{1}{r}$). This will be enough for our purposes. We now consider the field redefinition that transforms h_{CG} into h_{OS} , the on-shell Hamiltonian:

$$U = \exp \left(-\frac{i}{m_r} \{ \mathbf{W}(r), \mathbf{p} \} \right). \quad (92)$$

\mathbf{W} can be determined from the equation:

$$V_{ON}^{(1)} - V_{CG}^{(1)} = \frac{2}{m_r} \mathbf{W} \cdot (\nabla V^{(0)}). \quad (93)$$

Since the only possible tensor structure of \mathbf{W} is $\mathbf{W} = W(r^2) \mathbf{r}^i$ the above equation can be written as:

$$V_{ON}^{(1)} - V_{CG}^{(1)} = \frac{2}{m_r} W(r^2) \mathbf{r}^i \cdot (\nabla^i V^{(0)}). \quad (94)$$

We then obtain

$$\mathbf{W}^i = \frac{\pi}{2g_B^2} C_A (D_{CG}^{(1)} - D_{ON}^{(1)}) \frac{\mathbf{r}^i}{r^{1+2\epsilon}}, \quad (95)$$

and

$$h_{ON} = U^\dagger h_{CG} U = h_{CG} + \delta h = h^{(0)} + h_{ON}^{(2)} + h_{ON}^{(4)} + \dots \quad (96)$$

h_{CG} and h_{ON} obviously produce the same spectrum. Therefore, δh cannot produce energy shifts, and any change in the RG equations has to be compensated among different terms. Let us see how it works. $h_{ON}^{(2)}$ produces the differences reported in Eq. (88). Such differences should be eliminated by $h_{ON}^{(4)}$ (as the other contributions to the Hamiltonian are subleading), and indeed they do. In momentum space $\tilde{h}_{ON}^{(4)}$ reads

$$\begin{aligned} \tilde{h}_{ON}^{(4)} = & C_F^2 g_B^2 m_r \frac{\pi D_1^{(2)}}{8m_1^2 m_2^2} \left(|\mathbf{k}|^{1+2\epsilon} + 4(\mathbf{p} \cdot \mathbf{p}') |\mathbf{k}|^{-1+2\epsilon} + \frac{2(\mathbf{p} \cdot \mathbf{k})(\mathbf{p}' \cdot \mathbf{k})}{|\mathbf{k}|^{3-2\epsilon}} \right) \\ & + C_F \frac{\pi}{m_1 m_2} \left(-\frac{1}{4} C_F C_A D_{CG}^{(1)} + \frac{1}{4} \frac{m_r^2}{m_1 m_2} C_F^2 \frac{g_B^4}{16\pi^2} \right) \frac{g_B^2}{4\pi} \frac{1}{\epsilon} \frac{1}{|\mathbf{k}|^{-4\epsilon}} \\ & + \dots \end{aligned} \quad (97)$$

Note that the term proportional to $|\mathbf{k}|^{1+2\epsilon}$ in the first line gives a contribution to the potential RG equation through potential loops. It is equivalent to generating a new $1/m^3$ potential. The other two terms in the first line do not contribute to the potential RG equation. Looking at the 2nd line, it is also interesting to see that there is a kind of soft contribution, which nevertheless, has ultrasoft in the on-shell scheme. The second term in the second line can also be interpreted as a pure soft contribution. This brings the interesting observation that even if the potential RG equation can be written in a matching scheme independent way, the implicit scheme dependence of the potentials allows for a mixing with the soft computation (at least in the on-shell scheme). Finally, for the dots in the 3rd line we refer to extra contributions to $\tilde{h}_{ON}^{(4)}$, generated by the field redefinitions, which nevertheless do not contribute to the running.

References

- [1] A. Pineda and J. Soto, Nucl. Phys. Proc. Suppl. **64**, 428 (1998) [hep-ph/9707481].
- [2] N. Brambilla, A. Pineda, J. Soto and A. Vairo, Nucl. Phys. B **566**, 275 (2000) [hep-ph/9907240].
- [3] N. Brambilla, A. Pineda, J. Soto and A. Vairo, Rev. Mod. Phys. **77**, 1423 (2005) [hep-ph/0410047].
- [4] A. Pineda, Prog. Part. Nucl. Phys. **67** (2012) 735 [arXiv:1111.0165 [hep-ph]].
- [5] B. A. Kniehl, A. A. Penin, V. A. Smirnov and M. Steinhauser, Nucl. Phys. B **635**, 357 (2002) [hep-ph/0203166].
- [6] C. Peset, A. Pineda and M. Stahlhofen, JHEP **1605**, 017 (2016) [arXiv:1511.08210 [hep-ph]].

- [7] C. Peset, A. Pineda and J. Segovia, arXiv:1809.09124 [hep-ph].
- [8] A. Pineda, Phys. Rev. D **65**, 074007 (2002) [hep-ph/0109117].
- [9] B. A. Kniehl, A. A. Penin, A. Pineda, V. A. Smirnov and M. Steinhauser, Phys. Rev. Lett. **92**, 242001 (2004) Erratum: [Phys. Rev. Lett. **104**, 199901 (2010)] [hep-ph/0312086].
- [10] A. A. Penin, A. Pineda, V. A. Smirnov and M. Steinhauser, Phys. Lett. B **593**, 124 (2004) Erratum: [Phys. Lett. B **677**, no. 5, 343 (2009)] [hep-ph/0403080].
- [11] E. Eichten and B. Hill, Phys. Lett. **B243**, 427 (1990).
- [12] C. W. Bauer and A. V. Manohar, Phys. Rev. D **57**, 337 (1998) [hep-ph/9708306].
- [13] B. Blok, J. G. Korner, D. Pirjol and J. C. Rojas, Nucl. Phys. B **496**, 358 (1997) [hep-ph/9607233].
- [14] D. Moreno and A. Pineda, Phys. Rev. D **97**, no. 1, 016012 (2018) [arXiv:1710.07647 [hep-ph]].
- [15] G. Amorós, M. Beneke, and M. Neubert, Phys. Lett. B **401**, 81 (1997).
- [16] A. Czarnecki and A. G. Grozin, Phys. Lett. B **405**, 142 (1997) Erratum: [Phys. Lett. B **650**, 447 (2007)] [hep-ph/9701415].
- [17] N. Brambilla, A. Vairo, X. Garcia i Tormo and J. Soto, Phys. Rev. D **80**, 034016 (2009) [arXiv:0906.1390 [hep-ph]].
- [18] A. Pineda and M. Stahlhofen, Phys. Rev. D **84**, 034016 (2011) [arXiv:1105.4356 [hep-ph]].
- [19] A. Pineda, Phys. Rev. D **84**, 014012 (2011) [arXiv:1101.3269 [hep-ph]].
- [20] A. H. Hoang and M. Stahlhofen, Phys. Rev. D **75** (2007) 054025 [hep-ph/0611292].
- [21] A. H. Hoang and M. Stahlhofen, JHEP **1106**, 088 (2011) [arXiv:1102.0269 [hep-ph]].
- [22] J. Collins, Camb. Monogr. Part. Phys. Nucl. Phys. Cosmol. **32**, 1 (2011).
- [23] W. E. Caswell and G. P. Lepage, Phys. Lett. B **167**, 437 (1986).
- [24] G. T. Bodwin, E. Braaten and G. P. Lepage, Phys. Rev. D **51**, 1125 (1995) [Phys. Rev. D **55**, 5853 (1997)] [hep-ph/9407339].
- [25] A. V. Manohar, Phys. Rev. D **56**, 230 (1997) [hep-ph/9701294].
- [26] C. Balzereit, Phys. Rev. D **59**, 094015 (1999) [hep-ph/9805503].

- [27] X. Lobregat, D. Moreno and R. Petrossian-Byrne, Phys. Rev. D **97**, no. 5, 054018 (2018) [arXiv:1802.07767 [hep-ph]].
- [28] D. Moreno, Phys. Rev. D **98**, no. 3, 034016 (2018) [arXiv:1806.09323 [hep-ph]].
- [29] N. Brambilla, E. Mereghetti and A. Vairo, Phys. Rev. D **79**, 074002 (2009) [Phys. Rev. D **83**, 079904 (2011)] [arXiv:0810.2259 [hep-ph]].
- [30] R. J. Hill, G. Lee, G. Paz and M. P. Solon, Phys. Rev. D **87**, 053017 (2013) [arXiv:1212.4508 [hep-ph]].
- [31] A. Gunawardana and G. Paz, JHEP **1707**, 137 (2017) [arXiv:1702.08904 [hep-ph]].
- [32] C. Peset, A. Pineda and M. Stahlhofen, Eur. Phys. J. C **77**, no. 10, 681 (2017) [arXiv:1706.03971 [hep-ph]].
- [33] A. Pineda and J. Soto, Phys. Rev. D **58**, 114011 (1998) [hep-ph/9802365].
- [34] I. B. Khriplovich, A. I. Milstein and A. S. Yelkhovsky, Physica Scripta. Vol. T46, 252-260, 1993.
- [35] A. Czarnecki, K. Melnikov and A. Yelkhovsky, Phys. Rev. **A59**, 4316 (1999).
- [36] A. A. Penin, A. Pineda, V. A. Smirnov and M. Steinhauser, Nucl. Phys. B **699**, 183 (2004) Erratum: [Nucl. Phys. B **829**, 398 (2010)] [hep-ph/0406175].
- [37] A. Pineda and J. Soto, Phys. Rev. D **59**, 016005 (1999) [hep-ph/9805424].
- [38] M. Finkemeier and M. McIrvin, Phys. Rev. D **55**, 377 (1997) [hep-ph/9607272].
- [39] M. E. Luke and A. V. Manohar, Phys. Lett. B **286**, 348 (1992) [hep-ph/9205228].
- [40] A. V. Manohar and I. W. Stewart, Phys. Rev. Lett. **85**, 2248 (2000) [hep-ph/0004018].
- [41] M. E. Luke, A. V. Manohar and I. Z. Rothstein, Phys. Rev. D **61**, 074025 (2000) [hep-ph/9910209].
- [42] A. A. Penin and M. Steinhauser, Phys. Lett. B **538** (2002) 335 [hep-ph/0204290].
- [43] A. A. Penin, V. A. Smirnov and M. Steinhauser, Nucl. Phys. B **716**, 303 (2005) [hep-ph/0501042].
- [44] M. Beneke, Y. Kiyo and K. Schuller, Nucl. Phys. B **714**, 67 (2005) [hep-ph/0501289].
- [45] Y. Kiyo and Y. Sumino, Phys. Lett. B **730** (2014) 76 [arXiv:1309.6571 [hep-ph]].
- [46] Y. Kiyo and Y. Sumino, Nucl. Phys. B **889** (2014) 156 [arXiv:1408.5590 [hep-ph]].
- [47] N. Brambilla, A. Pineda, J. Soto and A. Vairo, Phys. Rev. D **63**, 014023 (2000) [hep-ph/0002250].